Copula-based Reliability Analysis of Degrading Systems with Dependent Failures

Guanqi Fang^a, Rong Pan^{a,≤}, Yili Hong^b

^aSchool of Computing, Informatics and Decision Systems Engineering, Arizona State University, Tempe, 85281, AZ

^bDepartment of Statistics, Virginia Tech, Blacksburg, 24061, VA

Abstract

Consider a coherent system, in which the degradation processes of its performance characteristics are positively correlated, this paper systematically investigates a bivariate degradation model of such a system. To analyze the accelerated degradation data, a flexible class of bivariate stochastic processes are proposed to incorporate the effects of environmental stress variables and the dependency between two degradation processes is modeled by a copula function. A two-step system reliability analysis approach is developed and it is implemented with the Hamiltonian Monte Carlo algorithm. Simulation studies validate this approach and the consequences of model misspecification are evaluated too. Furthermore, two real-world examples are presented to demonstrate the applicability of the proposed modeling framework of system reliability on correlated degradation processes.

Keywords: Accelerated Degradation Test, Bayesian Inference, Copula Function, Hamiltonian Monte Carlo, Multivariate Model, System Reliability

1. Introduction

1.1. Background

Complex engineering systems are built for fulfilling a myriad of functional requirements and simultaneous degradations of these system functions over time are common. For many systems, degradation is one of the main causes of system failure. In this paper, the degrading system we refer to is a single-component product with multiple performance characteristics (PCs). But the study we perform can be extended to a large scope, where the functions of multiple components in either a serial or a parallel system gradually deteriorate due to wears and tears, etc.

Over the past two decades, much work has been done on assessing system reliability based on the failure time data from life tests or accelerated life tests [1], and through data analysis, the system failure time distribution is estimated so as to predict system reliability. However, since many engineering systems are highly reliable and have more complex failure mechanisms, it is often technically challenging and costly to acquire lifetime data. Instead, the degradation tests (DTs) and accelerated degradation tests (ADTs), which collect the measurement data of the system's PCs, provide an efficient way for studying system aging. In recent years, utilizing degradation data to predict system reliability has become more important than ever before.

Email address: rong.pan@asu.edu (Rong Pan)

^{*}Corresponding author.

In literature, a degradation process over time, Y $t \neq \infty 1$, is often modeled through one of two major frameworks – the general path model and the stochastic process model. The general path model utilizes the regression technique to fit a degradation path function and, oftentimes, it is a model with random effects to account for unit-to-unit variability [2]. Some recent developments of the general path model include, e.g., [3–6]. Alternatively, the stochastic process model treats degradation measurements as the realization of a stochastic process, such as the Wiener process [7–9], Gamma process [10–12], and Inverse Gaussian process [13–15]. In most previous studies, researchers considered only a single PC; however, in reality, a system may consist of multiple PCs and there may exist dependencies among these PCs. If the dependencies among different degradation processes are ignored, some serious drawbacks, such as biases in system reliability prediction, can occur.

1.2. A Motivating Example

As a motivating example, a polymeric material degradation process is described in this section. The photodegradation caused by ultraviolet (UV) radiation is the primary cause of failure for polymeric materials [16]. In our daily life, this process commonly happens on the products with paints or coatings, such as automobile body, bridges, buildings, and some other outdoor structures. When such products are in use, many environmental factors (temperature, humidity, as well as UV spectrum and intensity) affect their performance. Meanwhile, the polymeric material's life is determined by several PCs, such as the benzene ring mass loss and the C-O stretching of aryl ether [17, 18]. Thus, to make a good assessment of this material's service life, it is necessary to conduct a multivariate analysis.

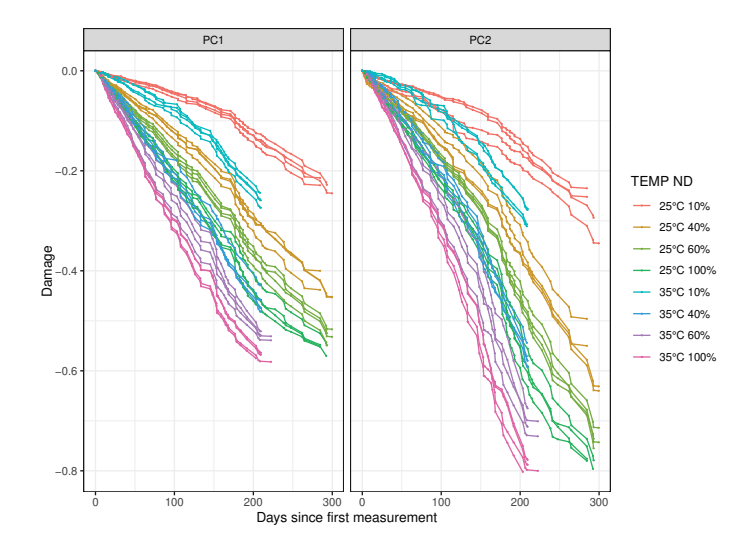


Figure 1: Degradation Path for Two PCs of Polymeric Material.

From 2002 through 2006, U.S. National Institute of Standards and Technology (NIST) conducted a few years of weathering experiments on organic coatings in both an indoor laboratory and some outdoor exposure facilities [19]. For the indoor experiment, they placed specimens in temperature/humidity-controlled chambers illuminated by controlled UV light. Ever since the experiments began, degradation was measured periodically at intervals of a few days using Fourier-transform infrared spectroscopy (FTIR) [20]. The heights of FTIR peaks correspond to the amount of particular chemical products and they have units cm⁻¹. Among the studied damage numbers, one of them was the peak at 1510 cm⁻¹, which corresponds to the benzene ring mass loss. Three other peaks being monitored contain 1250 cm⁻¹ (aromatic C-O), 1658 cm⁻¹ (oxidation products), and 2925 cm⁻¹ (CH mass loss). In this paper, we study two damage numbers – 1250 cm⁻¹, denoted by PC1, and 1510 cm⁻¹, denoted by PC2.

Failure is defined as the damage measurement exceeding a predetermined threshold. To accelerate the deterioration, various levels of external environmental variables were applied. From the indoor data we received, temperature (TEMP, in degrees Celsius °C) has two levels – 25°C and 35°C, and neutral density (ND), which is attributed to UV intensity, has four levels – 10%, 40%, 60%, and 100%. Figure 1 shows the degradation paths of two PCs from all test units at different combinations of stress variables. It can be seen that the acceleration effect brought by a stress is evident since each PC degrades faster as temperature or neutral density increases. Meanwhile, we notice that the two PCs share a similar degradation pattern even though the degradation of PC2 seems to be more advanced. This finding indicates that the degradation processes of two PCs could be correlated. Therefore, to evaluate the health of polymeric material, the following three modeling challenges must be addressed: 1) A flexible and reasonable bivariate degradation model is desired to account for the similarity and the distinction between the two PCs; 2) We need to deal with environmental variables and their effects on the degradation process; 3) An analytical approach to system reliability prediction needs to be established such that it can utilize the rich information contained in the degradation dataset.

1.3. Literature Review

The past related work on degradation-based system reliability analysis either assumes PCs are independent to each other or they are dependent with a known joint distribution. For example, Wang and Coit [21] introduced a multivariate normal distribution for the degradation processes of dependent components based on general path model. Pan and Balakrishnan [22] built a bivariate model based on Birnbaum Saunders distribution with gamma process as marginals. Wang et al. [23] adopted a nonlinear multivariate Wiener process (i.e., a multivariate normal distribution) to estimate remaining useful lifetime. Si et al. [24] implemented a multivariate general path model considering dynamic measurements. However, assigning a multivariate joint distribution to marginals may not be a suitable solution, as it is difficult to find an appropriate joint distribution in most cases especially when the marginal processes are subject to distinct distributions [25]. In such cases, a more flexible multivariate model is desired.

In recent years, the modeling of multiple degradation processes via copula function has gained a great deal attention, mostly due to the flexibility of copula function [26]. Copula is a tool to couple correlated marginal distributions to produce a new joint distribution. It is able to resolve two multivariate modeling difficulties – the existence of dependence between multiple PCs and the lack of closed-form multivariate distribution. For instance, Wang et al. [23] provided a modeling structure based on Gamma process via Frank copula. Peng et al. [27] proposed a bivariate modeling based on IG process via Gaussian copula and applied it on a degradation dataset from heavy machine tools. Pan et al. [28] applied Frank copula with Wiener process as marginals to the same dataset used in [22]. But the bivariate models proposed by these researchers all have the same stochastic process governing both marginals. Until recently, Peng et al. [29] utilized Wiener process and IG process to model a bivariate degradation process with both monotonic and non-monotonic paths. Rodríguez-Picón et al. [30] proposed a bivariate degradation model with marginal heterogeneous stochastic processes. Peng et al. [31] incorporated measurement error into stochastic process models with Gaussian copula. To our best knowledge, most previous work focused on the demonstration of some specific types of bivariate models (such as Frank copula with Gamma process in [32]). But there is still a lack of complete theoretical exposition to characterize the influence of PC dependence on system reliability with the copula approach. Furthermore, we notice that these literature usually took use of the traditional Metropolis algorithm to carry out statistical inference. However, it may not work well when dealing with problems with complex model structure and large data volume, such as the motivating example that involves several covariates and contains more than 4,111 data points.

1.4. Overview

In this paper, our objective is to develop a copula-based framework for analyzing a degrading system's reliability. This framework provides a general modeling approach for bivariate ADT data. In this approach, we separate the selection of marginal degradation process model and the construction of dependence structure between two marginal processes. Instead of the traditional Metropolis algorithm, a new computational Bayesian inference method, Hamiltonian Monte Carlo (HMC), is employed to estimate the unknown parameters in both marginal and joint models, and posterior samples are utilized to predict system reliability. We also provide two real-world examples to illustrate the proposed framework for system reliability analysis.

Three primary contributions have been made by this paper. First, we provide a systematic approach to investigating a degrading system's reliability in presence of dependent component failures. The results can be applied to general coherent serial and parallel systems. Second, we demonstrate the incorporation of covariate information into the proposed model. As discussed in Section 6.2, a quantitative analysis of the effects of covariates can be performed. Finally, based on the HMC algorithm, we develop an efficient Bayesian treatment to system reliability assessment, which differs from the traditional computational method used by other researchers.

The rest of the paper is organized as follows: Section 2 elaborates the modeling framework of a degrading system with dependent degradation processes. Section 3 introduces the specific models for bivariate degradation processes. It consists of Section 3.1, which provides the proposed general model structure, Section 3.2, which contains a detailed instruction of how to incorporate covariates into the model, and Section 3.3, which gives the marginal reliability function. In Section 4, the Bayesian approach to model parameter estimation is discussed. In Section 5, two simulation studies are carried out to assess the performance of the proposed inference method and to evaluate the consequences brought by model misspecification. Finally, two examples with real datasets are provided to demonstrate the workflow of the proposed degradation data analysis method in Section 6. Section 7 concludes the paper.

2. Copula Function and System Reliability Assessment

2.1. Degrading System with Multiple PCs

Consider a system with M components, or PCs, subject to degradation over time. Typically, we define a vector Y)t+[) Y_1) $t+Y_2$) $t+\dots, Y_M$)t+T to indicate the performance measurement for each PC at time t. Without loss of generality, we assume that Y_i)t+increases over time, j = 2, 3, ..., M. For instance, Y_i)t+may correspond to the fatigue-crack length of aluminum alloy [2]. Further denote a vector, $\boldsymbol{\omega}$ [) $\omega_1, \omega_2, \ldots, \omega_M \neq T$, representing the "soft failure" threshold; i.e. if Y_i) $t+\sim \omega_i$, the j^{th} PC is considered to be failed. In this paper, we consider a coherent system where the degradation of any PC will make the system less healthy. Meanwhile, we use \mathbf{R}) $t+[-)R_1$) $t+R_2$) $t+\ldots,R_M$)t+T to indicate the reliability for PC; i.e. R_i) $t+[P(Y_i)t+<\omega_i+j$ [2,3,..., M. Thus, the system reliability, R_s)t+ is defined as the probability that the system is functioning with R_s)t+[g)R)t+; where g is an increasing function of each R_i)t+for a coherent system. This implies that the system reliability is determined by the joint distribution of Y)t+ Two examples of coherent system include serial system and parallel system. For a serial system, the system reliability is given by R_s [$\int_{j=1}^{M} P(Y_j)t + \langle \omega_j + [$ $\int_{j=1}^{M} R_j t$ +if all PCs are independent with each other. Similarly, for a parallel system, the system reliability is given by R_s) $t+[2 \int_{j=1}^{M})2 P(Y_j)t+<\omega_j+[2 \int_{j=1}^{M})2 R_j)t+$ However, when the independent property is unrealistic, since it is often the case that there exist interactions between PCs, the aforementioned system reliability formulas are no longer valid. To describe this dependency, we introduce the concept of associated random variables as below:

Definition 1 [33]: A random d-vector, \mathbf{X} , is positively associated if the following inequality

$$E[g_1)X+g_2)X+\sim E[g_1)X+E[g_2)X+\hat{},$$

or equivalently,

$$Cov(g_1)\boldsymbol{X}+g_2)\boldsymbol{X}+\sim 1$$

holds for all real-value functions g_1 and g_2 , which are increasing (in each PC) and their expectations exist.

In this paper, we assume Y are positively associated because it is often the case that in reliability applications PCs are positively correlated. It can be easily seen that the equality holds when Y_j , $j \, [2, 3, ..., M$, are mutually independent for any increasing functions g_1 and g_2 . This implies that if the PCs are mutually independent in a system, the system reliability only depends on the marginal reliabilities R)t+ But when they are dependent, the system reliability is determined by both the marginal reliabilities and the dependence structure. Based on the definition, the following theorem summarizes the effect of PC dependency on the system reliability for both serial and parallel systems.

Theorem 1. Consider a degrading coherent system with M positively associated performance measurements at time t, i.e. $\mathbf{Y})t+[)Y_1)t+Y_2)t+\ldots,Y_M)t+\mathcal{T}$, $M\sim 3$. Let $\mathbf{R})t+[)R_1)t+R_2)t+\ldots,R_M)t+\mathcal{T}$ denote the marginal reliabilities at time t. Then the system reliability satisfies the following properties:

1. For a serial system,

2. For a parallel system,

n e
$$(R_1)t+R_2)t+\ldots, R_M)t+\geq R_s)t+\geq 2$$
 (2)

The proof for this theorem is provided in Appendix. From Theorem 1, one can see that when the performance measurements of PCs are positively associated, a general serial system is more reliable than a system with independent PCs, while the opposite is true for a general parallel system. To allow for modeling the dependence structure, we can take use of the idea of copula function, which will be explained in the next section.

2.2. Copula Function

A copula is the function that connects the joint distribution function with individual marginal distribution functions. It is defined as $C)u_1, u_2, \ldots, u_d+$; $]1, 2^d \propto]1, 2^{\hat{}}$, which is the joint cumulative density function (cdf) of a d-dimensional random vector on the unit cube $]1, 2^d$ with uniform marginal distributions. Mathematically, $C)u_1, u_2, \ldots, u_d+[-P)U_1 \geq u_1, U_2 \geq u_2, \ldots, U_d \geq u_d+$, where $U_j \rightarrow Unif)1, 2+\{j [-2,3,\ldots,d]$. These uniform marginal distributions may be transformed from other continuous distributions. The following theorem shows the connection between copula and a general multivariate distribution.

Sklar's Theorem [34]: Let $X = (x_1, x_2, \dots, x_d)$ be a random vector with marginal cdfs $(x_1, x_1, x_2, \dots, x_d)$ be their joint cdf. Define (x_j, x_j) be a random vector with marginal cdfs $(x_j, x_1, x_2, \dots, x_d)$ be their joint cdf. Define (x_j, x_j) be a random vector with marginal cdfs (x_j, x_j)

$$C)u_{1}, u_{2}, \dots, u_{d} + [C)F_{1}(x_{1} + F_{2})x_{2} + \dots, F_{d}(x_{d}) + [P)X_{1} \ge x_{1}, X_{2} \ge x_{2}, \dots, X_{d} \ge x_{d} + [H)x_{1}, x_{2}, \dots, x_{d} + (3)$$

With the cdf of a joint distribution, it is easy to derive its probability density function (pdf) as

$$h)x_1, x_2, \dots, x_d + [c)F_1(x_1 + F_2(x_2 + \dots, F_d(x_d + F_d(x_d$$

where $f_j(x_j)$ is the marginal pdf of X_j and $c(F_1)(x_1+F_2)(x_2+\dots,F_d)(x_d)$ is the copula density function, which can be obtained by taking partial derivative of copula function.

The survival function, \bigoplus \rtimes , as defined in [35] is given by

with $C_{i_1 i_2 \times \times k}(u_{i_1}, u_{i_2}, \dots, u_{i_k})$ +denoting the marginal of C related to (i_1, i_2, \dots, i_k) + For example, considering a bivariate case, Equation (5) becomes

$$(u_1, u_2 + [2 u_1 u_2 0 C)u_1, u_2 + [2 u_1 u_2 0 C)u_1, u_2 + [2 u_1 u_2 0 C)u_1]$$

Among all available copulas, there is a popular family of copulas called the Archimedean family. This family admits explicit formulas and they allow modeling variable dependence through an association parameter. In this paper, we consider the following four widely-used copulas in the Archimedean family: Gumbel copula, Frank copula, Clayton copula, and Joe copula. These copulas hold various types of tail dependence – Gumbel copula and Joe copula have upper tail dependence (λ_U), Clayton copula has lower tail dependence (λ_L), and Frank copula is symmetric with no tail dependence. Inside each of these copula functions, there is an association parameter, δ , which measures the dependency between two variables. The specific functions of these copulas are given as below:

- Gumbel copula: $C)u_1, u_2+[gx]$]) $\text{mi } u_1 \not = 0$) $\text{mi } u_2 \not = \frac{\delta}{\delta} \mid$, where $\delta \forall]2, \in +\text{and } \tau [2 2/\delta]$ with $\lambda_U [3 3^{1/\delta} \text{ and } \lambda_L [1;$
- Clayton copula: $C)u_1, u_2 + [\quad \text{n e} \quad))u_1^{\ \delta} \ 0 \ u_2^{\ \delta} \quad 2 + \frac{1}{\delta}, 1 \Big(, \text{ where } \delta \ \forall \] \quad 2, \in \ \# \}1 | \text{ and } \tau \ [\quad \frac{\delta}{2 + \delta} \text{ with } \lambda_U \ [\quad 1 \text{ and } \lambda_L \ [\quad 3^{-1/\delta};$
- Frank copula: $C)u_1, u_2 + [\frac{1}{\delta} \operatorname{mi} \left\{ \begin{array}{l} 2 \ 0 \ \frac{[\exp(-\delta u_1) \ 1][\exp(-\delta u_2) \ 1]}{\exp(-\delta) \ 1} \end{array} \right\} \sqrt{\text{where } \delta \ \forall \)} \in , 1 + \sum 1, \in + \text{and}$ $\tau \left[\begin{array}{c} 2 \ 0 \ 5 \frac{D_1(\delta) \ 1}{\delta} \ \text{with } D_1) \delta + [\begin{array}{c} \frac{1}{\delta} \bigcup \left\{ \frac{t}{e^t \ 1} dt \ \text{and} \ \lambda_U \left[\begin{array}{c} \lambda_L \left[\end{array} \right. 1; \end{array} \right] \right\} \right] = 0$
- Joe copula: C) $u_1, u_2+[2]$)2 $u_1 \stackrel{\delta}{+} 0$)2 $u_2 \stackrel{\delta}{+} 0$)2 $u_1 \stackrel{\delta}{+} 0$ 0 $u_2 \stackrel{\delta}{+} 0$ 0 where $\delta \forall]2, \in +$ with $\lambda_U [3 \quad 3^{1/\delta} \text{ and } \lambda_L [1.$

Note that the relationship between Kendall's correlation τ and the association parameter δ is also given for each of the copulas above. For Joe copula, τ can be approximated by Monte Carlo simulation [36].

2.3. System Reliability from Copula Viewpoint

Recall that when PCs are not mutually independent, the system reliability, R_s)t+, is determined by the joint distribution of \mathbf{Y})t+ By introducing the concept of copula, we can develop a straightforward, yet flexible, approach for constructing the joint distribution of \mathbf{Y})t+ More importantly, since the copula function generates this joint distribution via the cdfs of marginal random variables, it provides an intuitive method of combining marginal reliabilities and dependence structure to calculate the system reliability. Figure 2 illustrates the construction of bivariate joint distribution via a copula function, as well as the system reliability derived directly from a copula.

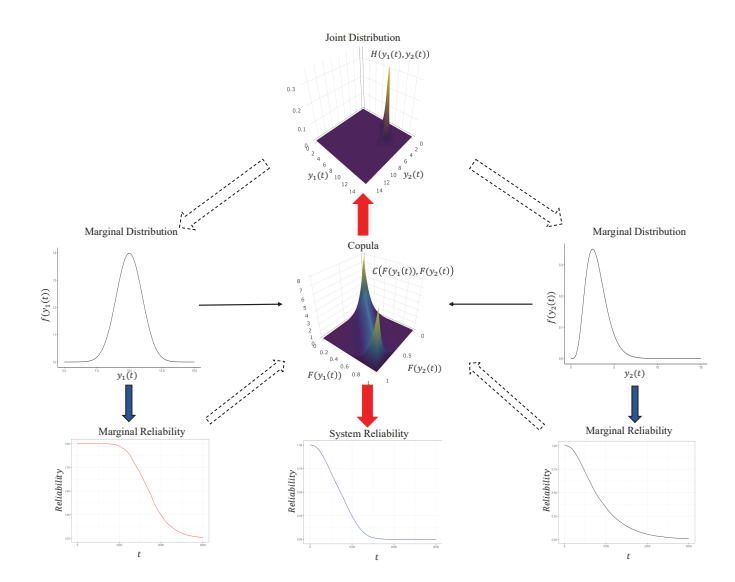


Figure 2: Construction of Bivariate Joint Distribution via Copula Function.

Therefore, from the copula perspective, the reliability of a degrading system with dependent PCs can be described by the following theorem:

Theorem 2. Consider a degrading coherent system with M positively associated performance measurements of components at time t, i.e. $\mathbf{Y})t+[)Y_1)t+Y_2)t+\ldots,Y_M)t+F$, $d\sim 3$. Let $\mathbf{R})t+[)R_1)t+R_2)t+\ldots,R_M)t+F$ denote the marginal reliabilities at time t. Then, the system reliability satisfies the following properties:

1. For a serial system,

$$R_s)t+[P(Y_1)t+<\omega_1,Y_2)t+<\omega_2,\ldots,Y_M)t+<\omega_M+$$

$$[CR_1)t+R_2)t+\ldots,R_M)t+\Theta^{Cop}(.$$
(6)

2. For a parallel system,

$$R_s)t+[2 P)Y_1)t+>\omega_1,Y_2)t+>\omega_2,\dots,Y_M)t+>\omega_M+$$

$$[2 R_1)t+R_2)t+\dots,R_M)t+\mathbf{\theta}^{Cop}\Big(.$$
(7)

where $\boldsymbol{\theta}^{Cop}$ is a set of parameters in the copula function.

Note that if all PCs are mutually independent, the system reliability is $\int_{j=1}^{M} R_j t$ +and $2 \int_{j=1}^{M} t t^2 dt$ as series system and a parallel system, respectively, and they can be derived from a independence copula, defined as $C(u_1, u_2, \dots, u_M) + \int_{j=1}^{M} u_j t^2 dt$.

It is also noticed that by introducing copula functions, three attractive features to data analysis are immediately obtained: 1) The marginal distributions of individual variables and their dependency structure can be separated. This feature will reduce the difficulty of parameter estimation. 2) There is no restriction on marginal model. It can be any distribution model that provides the best fit to the data. Thus, we will not be restricted to the same marginal distribution for different PCs. 3) The system reliability can be evaluated analytically once the marginal cdfs or marginal reliabilities are given. Therefore, utilizing a copula to characterize a degrading system will greatly facilitate the system reliability analysis.

3. Bivariate Degradation Process

3.1. A General Multivariate Model

Consider an ADT of N test units with M PCs. There are L environmental stress variables and K distinct time points when each test unit's degradation was measured. The degradation measurement is denoted by y_{ij} t_k +or y_{ijk} for the i^{th} test unit, j^{th} PC, and k^{th} time point, and the stress vector for each test unit is denoted by s_i . As a result, the degradation dataset for the j^{th} PC is given by

where s_i [) s_1, s_2, \ldots, s_L represents the values of stress variables for the i^{th} test unit and K_i is the total number of measurements for the i^{th} unit. K_i may vary from unit to unit. Under the stochastic process modeling framework, we work on degradation increments, which are defined as $\Lambda y_{ij})t_k+[y_{ij})t_k+y_{ij})t_k$ 1+ According to [37], the stochastic process modeling is favored than the general path modeling of degradation data because it is capable of including unexplainable randomness resided in the data, which may be caused by some unobserved environmental factors or some unknown effects of observed environmental factors. Based on the independent increment and infinite divisibility properties of Lévy process [38], a degradation dataset can be analyzed by using the following general multivariate model structure:

$$(\Delta Y_{i1}(t_k), \Delta Y_{i2}(t_k), \dots, \Delta Y_{iM}(t_k)) \to C \quad F_1(\Delta y_{i1}(t_k)), F_2(\Delta y_{i2}(t_k)), \dots, F_M(\Delta y_{iM}(t_k)); \boldsymbol{\theta}^{Cop}\Big(, \\ \Delta Y_{ij}(t_k) \to \text{MDP}(\boldsymbol{Y}_j; \boldsymbol{\theta}_j^{Mar}),$$
(8)

where C(x) is a copula function, representing the joint cdf of PCs, and $F_j(\Delta y_{ij}(t_k))$, $\boldsymbol{\theta}^{Cop}$, and $\boldsymbol{\theta}_j^{Mar}$ are the marginal cdf of individual PC, the parameters of copula function and the parameters of marginal degradation process (MDP), respectively. The MDPs in consideration here are Wiener process, Gamma process and Inverse Gaussian (IG) process, and they are given as follows:

$$MDP) \mathbf{Y}_{j} = \mathbf{\theta}_{j}^{Mar} + ; \begin{cases} \Lambda Y_{ij} t_{k} + \rightarrow N & \alpha_{j} h \right) \mathbf{s}_{i} + \Lambda \Phi_{j} t_{k} = \gamma_{j} + \beta_{j}^{2} h \right) \mathbf{s}_{i} + \Lambda \Phi_{j} t_{k} = \gamma_{j} + \beta_{j} + (1 + \alpha_{j}^{2} t_{k} + \cdots + \alpha_{j}^{2} t_{k} + \alpha_{j}^{2} t_{k} + \cdots + \alpha_{j}^{2} t_{k} + \alpha_{j}^{2} t_{k} = \gamma_{j} + \beta_{j} h \right) \mathbf{s}_{i} + \Lambda \Phi_{j} t_{k} = \gamma_{j} + \beta_{j} h \right) \mathbf{s}_{i} + \Lambda \Phi_{j} t_{k} = \gamma_{j} + \beta_{j} h \right) \mathbf{s}_{i} + \Lambda \Phi_{j} t_{k} = \gamma_{j} + \beta_{j} h \right) \mathbf{s}_{i} + \Lambda \Phi_{j} t_{k} = \gamma_{j} + \beta_{j} h \right) \mathbf{s}_{i} + \Lambda \Phi_{j} t_{k} = \gamma_{j} + \beta_{j} h \right) \mathbf{s}_{i} + \Lambda \Phi_{j} t_{k} = \gamma_{j} + \beta_{j} h \right) \mathbf{s}_{i} + \Lambda \Phi_{j} t_{k} = \gamma_{j} + \beta_{j} h \right) \mathbf{s}_{i} + \Lambda \Phi_{j} t_{k} = \gamma_{j} + \beta_{j} h \right) \mathbf{s}_{i} + \Lambda \Phi_{j} t_{k} = \gamma_{j} + \beta_{j} h \right) \mathbf{s}_{i} + \Lambda \Phi_{j} t_{k} = \gamma_{j} + \beta_{j} h \right) \mathbf{s}_{i} + \Lambda \Phi_{j} t_{k} = \gamma_{j} + \beta_{j} h \right) \mathbf{s}_{i} + \Lambda \Phi_{j} t_{k} = \gamma_{j} + \beta_{j} h \right) \mathbf{s}_{i} + \Lambda \Phi_{j} t_{k} = \gamma_{j} + \beta_{j} h \right) \mathbf{s}_{i} + \Lambda \Phi_{j} t_{k} = \gamma_{j} + \beta_{j} h \right) \mathbf{s}_{i} + \Lambda \Phi_{j} t_{k} = \gamma_{j} + \beta_{j} h \right) \mathbf{s}_{i} + \Lambda \Phi_{j} t_{k} = \gamma_{j} + \beta_{j} h \right) \mathbf{s}_{i} + \Lambda \Phi_{j} t_{k} = \gamma_{j} + \beta_{j} h \right) \mathbf{s}_{i} + \Lambda \Phi_{j} t_{k} = \gamma_{j} + \beta_{j} h \right) \mathbf{s}_{i} + \Lambda \Phi_{j} t_{k} = \gamma_{j} + \beta_{j} h \right) \mathbf{s}_{i} + \Lambda \Phi_{j} t_{k} = \gamma_{j} + \beta_{j} h \right) \mathbf{s}_{i} + \Lambda \Phi_{j} t_{k} = \gamma_{j} + \beta_{j} h \right) \mathbf{s}_{i} + \Lambda \Phi_{j} t_{k} = \gamma_{j} + \beta_{j} h \right) \mathbf{s}_{i} + \Lambda \Phi_{j} t_{k} = \gamma_{j} + \beta_{j} h \right) \mathbf{s}_{i} + \Lambda \Phi_{j} t_{k} = \gamma_{j} + \beta_{j} h \right) \mathbf{s}_{i} + \Lambda \Phi_{j} t_{k} = \gamma_{j} + \beta_{j} h \right) \mathbf{s}_{i} + \Lambda \Phi_{j} t_{k} = \gamma_{j} + \beta_{j} h$$

In Model (8), some popular copula functions, such as those from the Archimedean group, can be considered for modeling the dependence structure among PCs, while each MDP can be any one of the univariate processes listed in (9). To ease the mathematical notation, we use α and β to indicate the two parameters in a MDP and use $h) \not\rightarrow$ to represent a function of covariates in the marginal model. Finally, $\Lambda \Phi t_k = \gamma_j + [\Phi t_k = \gamma_j + \Phi t_k] + [\Phi t_k = \gamma_j + \Phi t_k]$, which is the time interval after a power transformation of original time with parameter γ_j .

Using this general modeling approach, a great amount of bivariate degradation models can be introduced. For instance, a bivariate degradation model with two different marginal processes, such as a Wiener process and an IG process, are demonstrated below:

$$)\Lambda Y_{i1})t_k + \Lambda Y_{i2})t_k + \longrightarrow C)F_1)\Lambda y_{i1})t_k + + F_2)\Lambda y_{i2})t_k + \Longrightarrow +,$$

$$\Lambda Y_{i1})t_k + \longrightarrow N \quad \alpha_1 \neq x) \quad \eta/s_i + \Phi_1)t = \gamma_1 + \beta_1^2 \neq x) \quad \eta/s_i + \Phi_1)t = \gamma_1 + \left(, \right.$$

$$\Lambda Y_{i2})t_k + \longrightarrow IG \quad \alpha_2 \neq x) \quad \eta/s_i + \Phi_2)t = \gamma_2 + \beta_2 \neq x) \quad \eta/s_i + \Phi_2)t = \gamma_1 + 2\left(.$$

$$(10)$$

Here, δ denotes the association parameter between two PCs. Specifically, for PC1, α_1 and β_1 represent the drift parameter and the diffusion parameter of a Wiener process, respectively. For PC2, α_2 and β_2 represent the mean and shape parameters of an IG process, respectively. In Model (10), we introduce a stress variable, s_i , to represent the stress level on the i^{th} test unit. If it is thermal stress, a simplified Arrhenius function can be used to capture the degradation acceleration effect of temperature. The detailed explanation of how to include a covariate in degradation analysis will be presented in the next section.

3.2. Covariate Information

When a product is highly reliable, its degradation rate could be too small to be noticeable under the normal use condition; thus, ADTs are adopted to expedite the degradation process by subjecting the product to some harsher environmental conditions, such as higher temperature or stronger vibration. Other common stress factors could be humidity, electric current, and voltage, etc. These stress factors are treated as covariates or markers in a statistical model [37]. To evaluate the effect of a covariate, Nelson [39] and Meeker and Escobar [2] discussed several acceleration functions that connect different types of stresses with a product's lifetime via the knowledge of chemical kinetics.

Five commonly used acceleration functions are listed in Table 1, where parameters ξ and η are product or material characteristics. These functions are indeed the link functions that incorporate the effects of corresponding covariates into a general degradation model. Note that an un-accelerated degradation test can be viewed as having h)s+[2. In engineering applications, choosing a good link function requires some domain knowledge of the underlying physical/chemical material change mechanism. In the literature, Doksum and Normand [40] used a linear link function to analyze biomaker data. Tang et al. [41] also assumed the linear link function and they applied it to analyze a LED dataset. Padgett and Tomlinson [42] declared that, when linking temperature to a Wiener process model, the power law function outperforms the Arrhenius function for analyzing a dataset of carbon-film resistor. When having more than one acceleration factor, Liao and Tseng [43] combined the Arrhenius function and the power law function to incorporate both temperature and electric current in their LED experiments, while Fang et al. [6] considered the Eyring function to integrate two stress variables, temperature and humidity.

In addition, finding an appropriate way to incorporate the link function into the degradation model structure requires the researcher to have a good understanding of the impact of stress factor on model parameter [37]. For example, to account for the degradation acceleration induced by temperature, Model (10) chooses a multiplicative effect derived from the Arrhenius law on the parameter; i.e.,

Table 1: Common Link Functions for Stress Acceleration Relations.

Acceleration Relation	Link Function				
Linear relation	$h)s+[\xi_0 \ 0 \ \xi_1 s]$				
Arrhenius relation	$h)s+[\xi e^{\eta/s}]$				
Power Law relation	$h)s+[\xi s^{\eta}]$				
Inverse-log relation	$h)s+[\xi)$ mi $s+\eta$				
Exponential relation	$h)s+[\xi e^{\eta s}]$				

 α_j g x) η/s_i + Furthermore, g x) η/s_i +and]g x) η/s_i +2 are incorporated into the diffusion parameter of Wiener process and the shape parameter of IG process, respectively. This indicates that a test unit under higher temperature will have a higher volatility in degradation. Nevertheless, there are a number of different ways to link parameters to stress variables. For instance, Park and Padgett [10] applied and compared four different link functions on analyzing a carbon-film resistor dataset and a fatigue crack size dataset. Peng [15] utilized the Arrhenius relation to involve explanatory variables into the Inverse Normal-Gamma mixture (ING) model and argued that it was a proportional mean model. Tang et al. [44] and Sun et al. [45] made use of the Arrhenius relation in modeling the drift parameter of a nonlinear Wiener process.

3.3. Marginal Reliability

For an individual PC, its marginal reliability function is relatively easy to obtain from a univariate stochastic process model. Without loss of generality, we let a degradation process start from Y)1+[1 and the failure time is the time when Y)t+first pass a threshold, ω . For example, Folks and Chhikara [46] proved that the first passage time (T_{ω}) of a Wiener process followed an inverse Gaussian distribution, IG) ω/α , ω^2/β^2 + The marginal reliability functions of the three stochastic processes listed in (9) are summarized as below:

• Wiener process

$$R)t+[P)T_{\omega} > t+[P)Y)t+<\omega+$$

$$\begin{bmatrix} 2 & - \end{bmatrix} \frac{2}{\beta} & \overline{\Phi})t = \gamma+ \\ h)s+ \\)\alpha h)s+\Phi)t = \gamma+ 2+\begin{cases} \\ \\ \\ \\ \end{bmatrix} \frac{3\alpha\omega}{\beta^{2}} \begin{bmatrix} - \end{bmatrix} \frac{2}{\beta} & \overline{\Phi})t = \gamma+\\ \\ (11)$$

• Gamma process

$$R)t + [P)T_{\omega} > t + [P)Y)t + < \omega +$$

$$[\frac{2}{\alpha h)s + \Phi}t = \gamma + (\alpha h)s + \Phi t = \gamma + \beta \omega (12)$$

• IG process

$$R)t+[P)T_{\omega} > t+[P)Y)t+<\omega+$$

$$\begin{bmatrix} - \end{bmatrix} \sqrt{\frac{\beta h)s+\Phi(t)}{\omega}} \frac{\partial \Phi(t)}{\partial t} \frac{\partial \Phi(t)}{\partial t} + 2 \begin{bmatrix} \{ \\ 0 \text{ g x } \end{bmatrix} \frac{\partial \Phi(t)}{\partial t} \frac{\partial \Phi(t)}{\partial t} + 2 \begin{bmatrix} \{ \\ 0 \text{ g x } \end{bmatrix} \frac{\partial \Phi(t)}{\partial t} \frac{\partial \Phi(t)}{\partial t} + 2 \begin{bmatrix} \{ \\ 0 \text{ g x } \end{bmatrix} \frac{\partial \Phi(t)}{\partial t} \frac{\partial \Phi(t)}{\partial t} + 2 \begin{bmatrix} \{ \\ 0 \text{ g x } \end{bmatrix} \frac{\partial \Phi(t)}{\partial t} \frac{\partial \Phi(t)}{\partial t} + 2 \begin{bmatrix} \{ \\ 0 \text{ g x } \end{bmatrix} \frac{\partial \Phi(t)}{\partial t} + 2 \begin{bmatrix} \{ \\ 0 \text{ g x } \end{bmatrix} \frac{\partial \Phi(t)}{\partial t} + 2 \begin{bmatrix} \{ \\ 0 \text{ g x } \end{bmatrix} \frac{\partial \Phi(t)}{\partial t} + 2 \begin{bmatrix} \{ \\ 0 \text{ g x } \end{bmatrix} \frac{\partial \Phi(t)}{\partial t} + 2 \begin{bmatrix} \{ \\ 0 \text{ g x } \end{bmatrix} \frac{\partial \Phi(t)}{\partial t} + 2 \begin{bmatrix} \{ \\ 0 \text{ g x } \end{bmatrix} \frac{\partial \Phi(t)}{\partial t} + 2 \begin{bmatrix} \{ \\ 0 \text{ g x } \end{bmatrix} \frac{\partial \Phi(t)}{\partial t} + 2 \begin{bmatrix} \{ \\ 0 \text{ g x } \end{bmatrix} \frac{\partial \Phi(t)}{\partial t} + 2 \begin{bmatrix} \{ \\ 0 \text{ g x } \end{bmatrix} \frac{\partial \Phi(t)}{\partial t} + 2 \begin{bmatrix} \{ \\ 0 \text{ g x } \end{bmatrix} \frac{\partial \Phi(t)}{\partial t} + 2 \begin{bmatrix} \{ \\ 0 \text{ g x } \end{bmatrix} \frac{\partial \Phi(t)}{\partial t} + 2 \begin{bmatrix} \{ \\ 0 \text{ g x } \end{bmatrix} \frac{\partial \Phi(t)}{\partial t} + 2 \begin{bmatrix} \{ \\ 0 \text{ g x } \end{bmatrix} \frac{\partial \Phi(t)}{\partial t} + 2 \begin{bmatrix} \{ \\ 0 \text{ g x } \end{bmatrix} \frac{\partial \Phi(t)}{\partial t} + 2 \begin{bmatrix} \{ \\ 0 \text{ g x } \end{bmatrix} \frac{\partial \Phi(t)}{\partial t} + 2 \begin{bmatrix} \{ \\ 0 \text{ g x } \end{bmatrix} \frac{\partial \Phi(t)}{\partial t} + 2 \begin{bmatrix} \{ \\ 0 \text{ g x } \end{bmatrix} \frac{\partial \Phi(t)}{\partial t} + 2 \begin{bmatrix} \{ \\ 0 \text{ g x } \end{bmatrix} \frac{\partial \Phi(t)}{\partial t} + 2 \begin{bmatrix} \{ \\ 0 \text{ g x } \end{bmatrix} \frac{\partial \Phi(t)}{\partial t} + 2 \begin{bmatrix} \{ \\ 0 \text{ g x } \end{bmatrix} \frac{\partial \Phi(t)}{\partial t} + 2 \begin{bmatrix} \{ \\ 0 \text{ g x } \end{bmatrix} \frac{\partial \Phi(t)}{\partial t} + 2 \begin{bmatrix} \{ \\ 0 \text{ g x } \end{bmatrix} \frac{\partial \Phi(t)}{\partial t} + 2 \begin{bmatrix} \{ \\ 0 \text{ g x } \end{bmatrix} \frac{\partial \Phi(t)}{\partial t} + 2 \begin{bmatrix} \{ \\ 0 \text{ g x } \end{bmatrix} \frac{\partial \Phi(t)}{\partial t} + 2 \begin{bmatrix} \{ \\ 0 \text{ g x } \end{bmatrix} \frac{\partial \Phi(t)}{\partial t} + 2 \begin{bmatrix} \{ \\ 0 \text{ g x } \end{bmatrix} \frac{\partial \Phi(t)}{\partial t} + 2 \begin{bmatrix} \{ \\ 0 \text{ g x } \end{bmatrix} \frac{\partial \Phi(t)}{\partial t} + 2 \begin{bmatrix} \{ \\ 0 \text{ g x } \end{bmatrix} \frac{\partial \Phi(t)}{\partial t} + 2 \begin{bmatrix} \{ \\ 0 \text{ g x } \end{bmatrix} \frac{\partial \Phi(t)}{\partial t} + 2 \begin{bmatrix} \{ \\ 0 \text{ g x } \end{bmatrix} \frac{\partial \Phi(t)}{\partial t} + 2 \begin{bmatrix} \{ \\ 0 \text{ g x } \end{bmatrix} \frac{\partial \Phi(t)}{\partial t} + 2 \begin{bmatrix} \{ \\ 0 \text{ g x } \end{bmatrix} \frac{\partial \Phi(t)}{\partial t} + 2 \begin{bmatrix} \{ \\ 0 \text{ g x } \end{bmatrix} \frac{\partial \Phi(t)}{\partial t} + 2 \begin{bmatrix} \{ \\ 0 \text{ g x } \end{bmatrix} \frac{\partial \Phi(t)}{\partial t} + 2 \begin{bmatrix} \{ \\ 0 \text{ g x } \end{bmatrix} \frac{\partial \Phi(t)}{\partial t} + 2 \begin{bmatrix} \{ \\ 0 \text{ g x } \end{bmatrix} \frac{\partial \Phi(t)}{\partial t} + 2 \begin{bmatrix} \{ \\ 0 \text{ g x } \end{bmatrix} \frac{\partial \Phi(t)}{\partial t} + 2 \begin{bmatrix} \{ \\ 0 \text{ g x } \end{bmatrix} \frac{\partial \Phi(t)}{\partial t} + 2 \begin{bmatrix} \{ \\ 0 \text{ g x } \end{bmatrix} \frac{\partial \Phi(t)}{\partial t} + 2 \begin{bmatrix} \{ \\ 0 \text{ g x } \end{bmatrix} \frac{\partial \Phi(t)}{\partial t} + 2 \begin{bmatrix} \{ \\ 0 \text{ g x } \end{bmatrix} \frac{\partial \Phi(t)}{\partial t} + 2 \begin{bmatrix} \{ \\ 0 \text{ g x } \end{bmatrix} \frac{\partial \Phi(t)}{\partial t} + 2 \begin{bmatrix} \{ \\ 0 \text{ g x } \end{bmatrix} \frac{\partial \Phi(t)}{\partial t} + 2 \begin{bmatrix} \{ \\ 0 \text{ g x } \end{bmatrix} \frac{\partial \Phi(t)}{\partial t} + 2 \begin{bmatrix} \{ \\ 0 \text{ g x } \end{bmatrix} \frac{\partial \Phi(t)}{\partial t} + 2 \begin{bmatrix} \{ \\ 0 \text{ g x } \end{bmatrix} \frac{\partial \Phi(t)}{\partial t$$

Here, Φ) $t=\gamma+[t^{\gamma}]$, a power transformation on the time scale.

4. Bayesian Approach to System Reliability Analysis

In Sections 2 and 3, we provide an overview of system reliability analysis with generally dependent degradation PCs. To systematically analyze a product with multiple, generally correlated, degrading PCs, we propose a two-step Bayesian approach, which is illustrated by a flowchart in Figure 3. In the first step our goal is to select the best multivariate degradation model to fit the data and to infer model parameters. Then, in the second step we utilize the posterior samples of model parameters to conduct system reliability analysis.

Step 1: Degradation Modeling and Parameter Estimation

When a bivariate degradation process is modeled by the modeling framework as in (8), we may group these model parameters as $\boldsymbol{\theta}_1^{Mar} \left[\right] \alpha_1, \beta_1, \gamma_1, \boldsymbol{\eta}_1^{\text{op}}, \boldsymbol{\theta}_2^{Mar} \left[\right] \alpha_2, \beta_2, \gamma_2, \boldsymbol{\eta}_2^{\text{op}},$ and $\boldsymbol{\theta}^{Cop} \left[\right] \delta$. Thus, the log-likelihood function is given by

$$\operatorname{m} L)\boldsymbol{\theta}_{1}^{Mar}, \boldsymbol{\theta}_{2}^{Mar}, \boldsymbol{\theta}^{Cop} + \left[\prod_{i=1}^{N} \prod_{k=1}^{K_{i}} \operatorname{m} c F_{1} \right] \Lambda y_{i1} t_{k} + \boldsymbol{\theta}_{1}^{Mar} + F_{2} \Lambda y_{i2} t_{k} + \boldsymbol{\theta}_{2}^{Mar} + \boldsymbol{\theta}^{Cop} \left(\prod_{i=1}^{N} \prod_{j=1}^{2} \prod_{k=1}^{K_{i}} \operatorname{m} f_{j} \right) \Lambda y_{ij} t_{k} + \boldsymbol{\theta}_{j}^{Mar} + \left(14 \right) \right]$$

It is difficult to directly maximize Equation (14) so as to find the maximum likelihood estimation (MLE) of model parameters. However, the separation of marginals and copula density suggests that we can firstly estimate the marginal parameters and then infer the copula association parameter, leading to a two-stage approach. The basic idea of this approach originates from the work provided by Joe [47]. However, if the problem has a complex data structure and large data size (e.g., the motivating example aforementioned contains more than 4,111 data points), it is difficult find a numerically stable solution by MLE. Instead, by leveraging the flexibility of computational Bayesian methods, we develop a Bayesian version of the two-stage inference technique. This two-stage Bayesian inference method is illustrated in the upper part of Figure 3.

First, we select the best marginal model for each PC. The univariate models listed in (9) are considered as potential candidates. Following the Bayesian inference method, the mathematical expression of posterior distribution of MDP parameters is given by

$$p)\boldsymbol{\theta}_{j}^{Mar} \boldsymbol{Y_{j}} + \infty \pi)\boldsymbol{\theta}_{j}^{Mar} + \equiv f)\boldsymbol{Y_{j}} \boldsymbol{\theta}_{j}^{Mar} + \\ \infty \pi)\boldsymbol{\theta}_{j}^{Mar} + \equiv f)\Lambda y_{ij} t_{k} + \boldsymbol{\theta}_{j}^{Mar} + j \left[2, 3. \right]$$

$$(15)$$

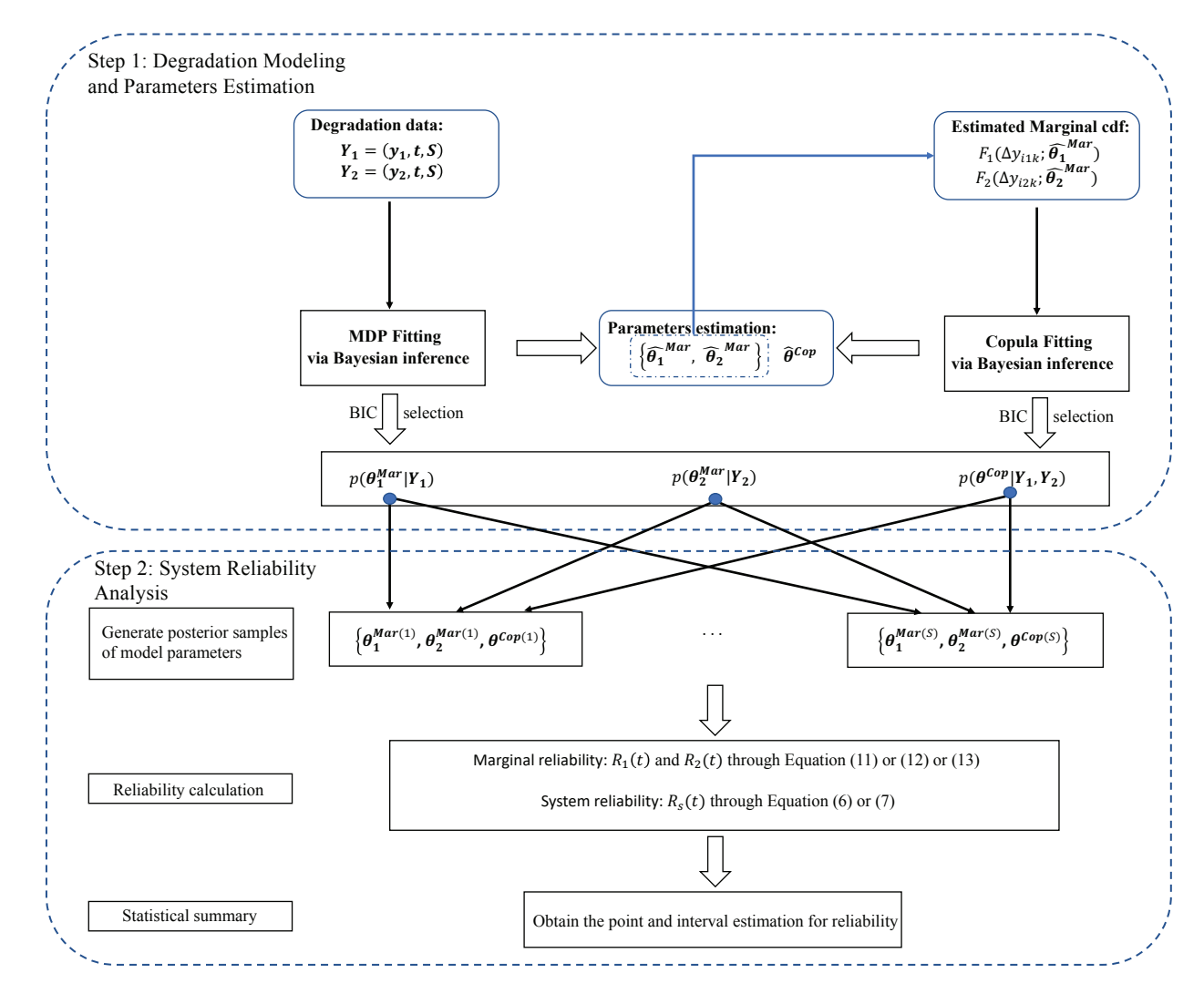


Figure 3: Flowchart of Two-step Bayesian Approach for System Reliability Analysis.

After the parameters embedded in each model are estimated, the Bayesian Information Criterion (BIC), which is given below, can be employed to compare their goodness-of-fit:

$$BIC = 3 \text{ m} \text{ } 2 + 0 \text{ } p \text{ m} \text{ } n + 1$$

where p and n are the number of parameters and the sample size, respectively.

Next, we select the best joint model via copula functions. Based on the marginal models determined in the first stage, the corresponding pairs of cdfs for degradation increments, F_1) $\Lambda y_{i1k} = \theta_1 + F_2$) $\Lambda y_{i2k} = \theta_2 + F_3$ are computed and they are treated as sample data for inferring copula functions. By the Bayesian approach, the posterior distribution of copula parameter is given by

$$p)\boldsymbol{\theta}^{Cop} \mathbf{Y}_{1}, \mathbf{Y}_{2} + \infty \pi)\boldsymbol{\theta}^{Cop} + \equiv \sum_{i=1}^{N} c \int_{k=1}^{K_{i}} c \int_{k=1}^{K_{i}} f(x) \int_{k=1}^{K_{i}} f(x) \int_{k=1}^{Mar} f(x$$

To construct these posterior distributions as formulated in Equations (15) and (16), we need to employ the Markov chain Monte Carlo (MCMC) technique to generate the posterior samples of parameters of interest and to obtain the point or interval estimations by summarizing these posterior

samples. Several previous publications, including [28], [29], and [48], utilized the well-known Metropolis algorithm, which is described below.

Algorithm 1: Metropolis Algorithm [49] Given a current sample $\theta^{(s)}$, a new sample $\theta^{(s+1)}$ is obtained as follows:

- 1. Sample $\theta^{\leq} \to J)\theta \theta^{(s)}$ where J is a proposal distribution;
- 2. Compute the acceptance ratio

$$r \begin{bmatrix} \frac{p)\boldsymbol{\theta}^{\leq}Data+}{p)\boldsymbol{\theta}^{(s)}Data+} \begin{bmatrix} \frac{\pi)\boldsymbol{\theta}^{\leq}+L)\boldsymbol{\theta}^{\leq}Data+}{\pi)\boldsymbol{\theta}^{(s)}+L)\boldsymbol{\theta}^{(s)}Data+} \end{bmatrix}$$

where *Data* represents a set of observed data points.

3. Let

$$\boldsymbol{\theta}^{(s+1)} \begin{bmatrix} \boldsymbol{\theta}^{\leq} \text{ with probability n lo} \\ \boldsymbol{\theta}^{(s)} \text{ with probability } 2 \text{ n lo} \end{pmatrix} r, 2+$$

This step can be accomplished by sampling $u \to Uniform)1, 2+$ and setting $\boldsymbol{\theta}^{(s+1)} [\boldsymbol{\theta}^{\leq}, \text{ if } u < r, \text{ and setting } \boldsymbol{\theta}^{(s+1)} [\boldsymbol{\theta}^{(s)}, \text{ otherwise.}]$

In those papers, the BUGS family of Bayesian inference platforms [50] were used. The BUGS software typically sets the proposal distribution, J, as either a multivariate normal distribution or several univariate normal distributions centering at the current sample. Essentially, the Metropolis algorithm presents a random-walk behavior, which results in inefficiency when exploring a high-dimensional posterior surface. For example, the running time of Algorithm 1 until convergence for the aforementioned motivating example will be extremely long. To expedite the inference process, we choose another family of MCMC algorithms called the Hamiltonian Monte Carlo (HMC). Being closely related to the Hamiltonian mechanics, HMC treats the parameter of interest, θ_{d*1} , as a position variable and introduces an auxiliary variable, p_{d*1} , as a momentum variable. Meanwhile, the potential energy is defined as the negative posterior log-likelihood, i.e. $U)\theta+[$ $\text{m }L)\theta$ Data+, and the kinetic energy is defined as $K)p+[\frac{p^Tp}{2}]$. According to the property of energy conservation of Hamiltonian dynamics, the Hamiltonian function, $H(\theta, p+[U(\theta+0)]K(p+1)$ should remain invariant along the whole period of movement. In other words, under the framework of a Hamiltonian system, the energy is mutually transferred between the potential energy and the kinetic energy with the change of system state. In terms of determining $P(\theta, p)$, which is the probability indicating the system being at a certain state θ, p + the concept of a canonical distribution from statistical mechanics can be applied. This is given by

$$P)\boldsymbol{\theta}, \boldsymbol{p} + \begin{bmatrix} \frac{2}{Z} g & x \end{pmatrix} \frac{H)\boldsymbol{\theta}, \boldsymbol{p} + \begin{bmatrix} \\ T \end{bmatrix}}{T} \begin{bmatrix} \frac{2}{Z} g & x \end{pmatrix} \frac{U)\boldsymbol{\theta} + \begin{bmatrix} \\ T \end{bmatrix}}{T} \begin{bmatrix} g & x \end{pmatrix} \frac{K)\boldsymbol{p} + \begin{bmatrix} \\ T \end{bmatrix}}{T} \begin{bmatrix} \frac{2}{Z}\pi)\boldsymbol{\theta} + L)\boldsymbol{\theta} \ Data + g & x \end{pmatrix} \frac{K}{T} \begin{bmatrix} \frac{K}{Z}\pi)\boldsymbol{\theta} + L \end{bmatrix} \begin{bmatrix} \frac{2}{Z}\pi + L \end{bmatrix}$$

where Z is a normalizing constant, and T is the temperature of the system and it can be assumed to be 2. In summary, the HMC algorithm is given by Algorithm 2 below.

Algorithm 2: HMC Algorithm [51]

Given a current sample $\boldsymbol{\theta}^{(s)}$, a new sample $\boldsymbol{\theta}^{(s+1)}$ is obtained as follows:

- 1. Sample $\boldsymbol{p}^{(s)} \to N)\mathbf{0}, \boldsymbol{I} +$
- 2. Run Leapfrog algorithm at $\theta^{(s)}$, $p^{(s)}$ +for L steps with step size ϵ to obtain proposed state θ^{\leq} , p^{\leq} +
 - 2.1 Make a half step for momentum at the beginning:

$$p_i^{\leq}[p_i^{\leq}] \epsilon/3 + \frac{\partial U}{\partial \theta_i} \theta^{(s)} + \{i [2, \dots, d.$$

2.2 Alternate L times with full step for position:

$$\theta_i^{\leq}[\quad \theta_i^{(s)} \ 0 \ \epsilon p_i^{\leq}, \ \{i \ [\quad 2, \dots, d.$$

2.3 Make a half step for momentum at the end:

$$p_i^{\leq}[\begin{array}{cc}p_i^{\leq}\end{array}]\epsilon/3+\frac{\partial U}{\partial\theta_i})\boldsymbol{\theta}^{\leq}+, \ \{i\ [2,\ldots,d.$$

Then,
$$\boldsymbol{\theta}^{\leq}[)\theta_{1}^{\leq},\theta_{2}^{\leq},\ldots,\theta_{d}^{\leq}+\text{and}\boldsymbol{p}^{\leq}[)p_{1}^{\leq},p_{2}^{\leq},\ldots,p_{d}^{\leq}+$$

Thus, $H)\boldsymbol{\theta}^{(s)},\boldsymbol{p}^{(s)}+[U)\boldsymbol{\theta}^{(s)}+0K)\boldsymbol{p}^{(s)}+\text{and}H)\boldsymbol{\theta}^{\leq},\boldsymbol{p}^{\leq}+[U)\boldsymbol{\theta}^{\leq}+0K)\boldsymbol{p}^{\leq}+$

3. Compute the acceptance ratio

$$r \left[\begin{array}{cc} P) \boldsymbol{\theta}^{\leq}, \boldsymbol{p}^{\leq} + \\ P) \boldsymbol{\theta}^{(s)}, \boldsymbol{p}^{(s)} + \end{array} \right] \left[\begin{array}{cc} \mathbf{g} \ \mathbf{x} \end{array} \right] H) \boldsymbol{\theta}^{(s)}, \boldsymbol{p}^{(s)} + \end{array} H) \boldsymbol{\theta}^{\leq}, \boldsymbol{p}^{\leq} + \left[\begin{array}{cc} \pi) \boldsymbol{\theta}^{\leq} + L) \boldsymbol{\theta}^{\leq} Data + N) \boldsymbol{p}^{\leq} \mathbf{0}, \boldsymbol{I} + \\ \pi) \boldsymbol{\theta}^{(s)} + L) \boldsymbol{\theta}^{(s)} Data + N) \boldsymbol{p}^{(s)} \mathbf{0}, \boldsymbol{I} + \end{array} \right] = 0$$

where *Data* represents a set of observed data points.

4. Let

$$\boldsymbol{\theta}^{(s+1)} \begin{bmatrix} \boldsymbol{\theta}^{\leq} \text{ with probability n lo} \\ \boldsymbol{\theta}^{(s)} \text{ with probability 2 n lo} \\ r, 2+ \end{cases}$$

This step can be accomplished by sampling $u \to Uniform)1, 2+$ and setting $\boldsymbol{\theta}^{(s+1)}$ [$\boldsymbol{\theta}^{\leq}$ if u < r and setting $\boldsymbol{\theta}^{(s+1)}$ [$\boldsymbol{\theta}^{(s)}$ otherwise.

In Algorithm 2, the Leapfrog algorithm at Step 2 is a method of numerical approximation to calculate $\boldsymbol{\theta}$ and \boldsymbol{p} according to the Hamiltonian equations. HMC differs from the Metropolis algorithm on two aspects: 1) HMC adds two normal densities into the acceptance ratio calculation. This may look like a trivial difference, but the resulted ratio value of HMC is much higher due to the subtle difference between H) $\boldsymbol{\theta}^{(s)}$, $\boldsymbol{p}^{(s)}$ +and H) $\boldsymbol{\theta}^{\leq}$, \boldsymbol{p}^{\leq} +, which is purely caused by the approximation error of Leapfrog algorithm. In fact, there should be no change due to the property of energy conservation of Hamiltonian system. Thus, with a higher sample acceptance rate, HMC is more efficient than the Metropolis algorithm. 2) Apparently, in Step 2 of the HMC algorithm, the gradient of posterior distribution is utilized to generate new momentum variable, \boldsymbol{p} . The Metropolis algorithm simply uses a proposal distribution that is not directly related to the target distribution. Thus, given an equal length of running steps, HMC should reach to the steady state much sooner than the Metropolis algorithm.

HMC is able to find a lower value of negative log-likelihood in fewer number of iterations and has the autocorrelation of samples decayed much faster [52]. In this paper, we use a HMC software package called RStan [53]. In addition, we use non-informative prior distributions, such as uniform distributions within relatively large intervals.

Step 2: System Reliability Analysis

After the joint degradation model was established, the system reliability is to be calculated. The lower part of Figure 3 shows the procedure of reliability prediction. Given the posterior samples of model parameters after a burn-in period, a total number of S samples are drawn. Then, the marginal and system reliability are calculated based on Equations (11) to (13) and Equations (6) and (7), respectively. Again, using these samples, both the point and interval estimation of reliability can be obtained.

5. Simulation Study

5.1. Performance of the Proposed Inference Method

In this section, we conduct a Monte Carlo simulation study to demonstrate the performance of the proposed two-stage system reliability analysis approach. For illustration, we simulate three different bivariate models with heterogeneous marginals and they are the Frank copula with Wiener-Gamma combination (Simulation Model %2 or SM%2), the Gumbel copula with Gamma-IG combination (SM%3), and the Clayton copula with Wiener-IG combination (SM%4).

$$SM\%2;)\Lambda Y_{i1})t_k+, \Lambda Y_{i2})t_k++\rightarrow C_{Frank})F_1)\Lambda y_{i1})t_k++, F_2)\Lambda y_{i2})t_k++=21+,$$

$$\Lambda Y_{i1})t_k+\rightarrow N)2.6\Lambda t_k, 1.6^2\Lambda t_k+,$$

$$\Lambda Y_{i2})t_k+\rightarrow Ga)4\Lambda t_k, 3+,$$

$$SM\%3;)\Lambda Y_{i1})t_k+, \Lambda Y_{i2})t_k++\rightarrow C_{Gumbel})F_1)\Lambda y_{i1})t_k++, F_2)\Lambda y_{i2})t_k++=4+,$$

$$\Lambda Y_{i1})t_k+\rightarrow Ga)5\Lambda t_k, 4+,$$

$$\Lambda Y_{i2})t_k+\rightarrow IG)3\Lambda t_k, 6\Lambda t_k^2+,$$

$$SM\%4;)\Lambda Y_{i1})t_k+, \Lambda Y_{i2})t_k++\rightarrow C_{Clayton})F_1)\Lambda y_{i1})t_k++, F_2)\Lambda y_{i2})t_k+=3+,$$

$$\Lambda Y_{i1})t_k+\rightarrow N)3\Lambda t_k, 1.4^2\Lambda t_k+,$$

$$\Lambda Y_{i2})t_k+\rightarrow IG)2.6\Lambda t_k, 5\Lambda t_k^2+,$$

where $\Lambda t_k \begin{bmatrix} t_k & t_{k-1} \end{bmatrix}$.

Algorithm 3: Random Degradation Value Generation

```
1. for i [ 2 to N do

2. for k [ 2 to K do

3. Generate )u_1, u_2 + \text{from } C)u_1, u_2 \delta +

4. Calculate \Lambda y_{ijk} through F_j^{-1})u_j \theta_j^{Mar}) for j [ 2, 3

5. Set y_{ijk} [ y_{ij,k-1} 0 \Lambda y_{ijk}, where y_{ij0} [ 1 for j [ 2, 3

6. end for

7. end for
```

To ease the computational burden, we set $N[2, h]s+[2, \Phi]t+[t]$ and the number of degradation measurements to be K[41, 66, or 91]. We repeat each simulated process 2,111 times. To initialize

the simulation procedure, an algorithm (see the pseudocode in Algorithm 3) for generating random degradation values is implemented. Then, on each replicate, the two-stage system analysis method is applied. Finally, an indicator variable, stating whether or not the true parameters are covered by the :6(credible interval, is recorded, as well as the sample mean of the estimated parameter values.

The simulation bias, standard deviation (SD) and coverage probability (CP) for each parameter in SM%2 are shown in Figure 4. Due to the space limitation, the results for SM%3 and SM%4 are presented in the supplementary document. As expected, the 95% credible interval for each parameter in each model has its CP value around its nominal level for all sample sizes. Also, the simulation biases and SDs decrease as the sample size increases, except for the bias of δ estimate in SM%3, where the estimation values at three scenarios remain at the same level. This is due to the small sample size and it is not a big concern. Therefore, when dealing with the real example that has a larger sample size, the inference method that we used here should perform more effectively on estimating model parameters.

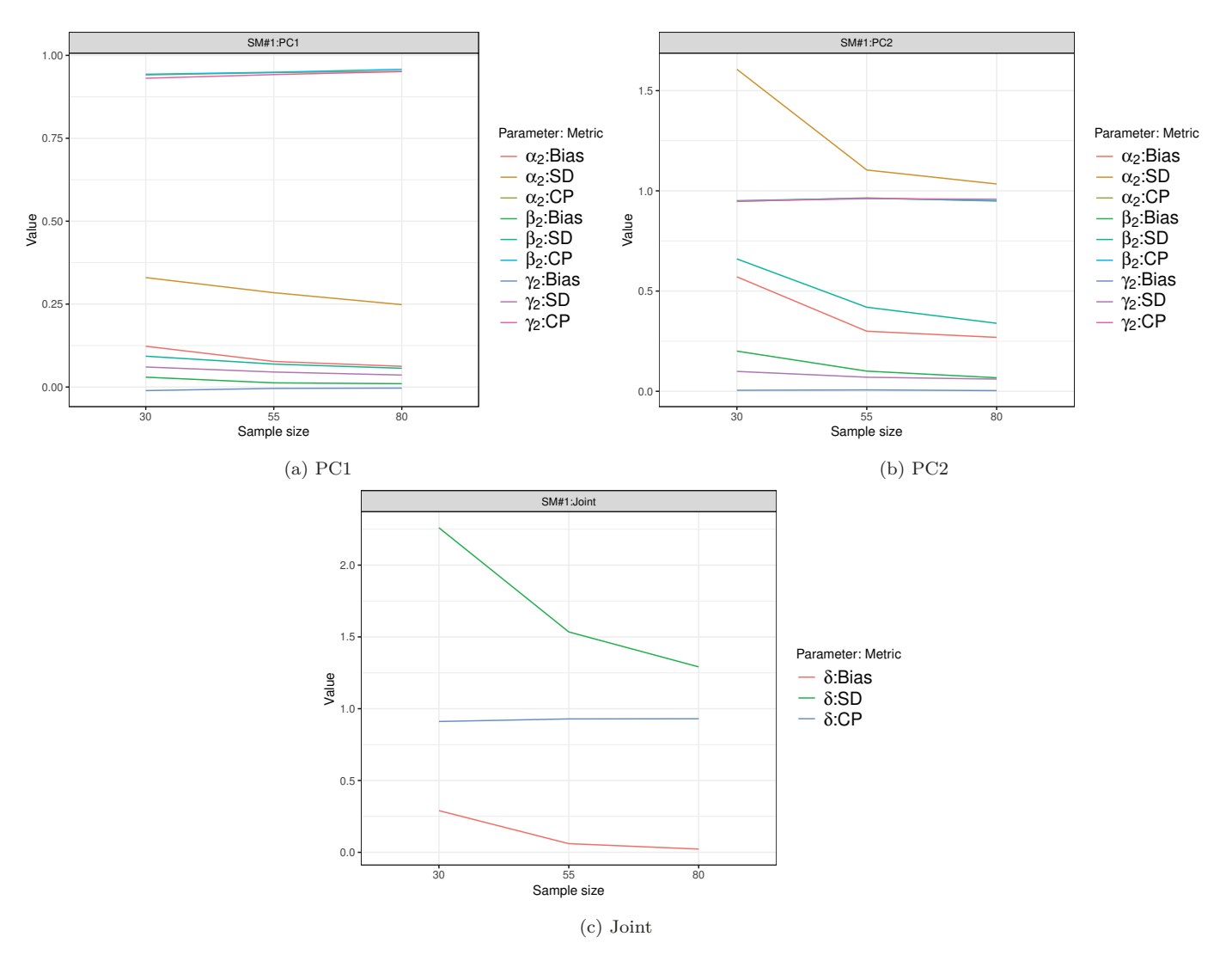


Figure 4: Monte Carlo Simulation Results for SM#1

5.2. Model Misspecification

As mentioned in the literature review, most previous works on bivariate degradation models assumed the same type of stochastic process model for both PCs. Among these models, the Wiener

processes with various copula functions are often employed due to its close relationship with normal distribution. However, if the combination of a non-monotonic process and a monotonic process, such as the Wiener-Gamma combination, is present, accepting the Wiener-Wiener model a priori without an examination of data may result in a bad joint distribution model. In this simulation study, we simulate three degradation processes that are generated by the Wiener-Gamma combination with various copulas and parameters. To reduce the variability caused by simulation, we set N [41 and K [41, leading to a relatively large sample size. Similarly to the previous study, we let h)s+[2. The degradation data are generated from models SM%5, SM%6, and SM%7 using the parameter values as shown below. Specifically, we set the power transformation to be as Φ) t_k = γ +[t_k^{γ} t_k^{γ} 1, where γ controls the time scale. Different γ values (being less than or greater than 2) will adjust the shape of degradation path (i.e., convex, linear, or concave). In addition, Gumbel copula, Frank copula and Clayton copula are applied to realize various types of degradation process dependency. The results of parameter estimation are included in the supplementary document.

$$SM\%5;)\Lambda Y_{i1})t_k+, \Lambda Y_{i2})t_k++\to C_{Gumbel})F_1)\Lambda y_{i1})t_k++, F_2)\Lambda y_{i2})t_k++=4+, \\ \Lambda Y_{i1})t_k+\to N)2.6\Phi)t_k=1.7+, 1.6^2\Phi)t_k=1.7++, \\ \Lambda Y_{i2})t_k+\to Ga)4\Phi)t_k=1.6+, 3+, \\ SM\%6;)\Lambda Y_{i1})t_k+, \Lambda Y_{i2})t_k++\to C_{Frank})F_1)\Lambda y_{i1})t_k++, F_2)\Lambda y_{i2})t_k++=3+, \\ \Lambda Y_{i1})t_k+\to N)2.6\Phi)t_k=2+, 1.6^2\Phi)t_k=2++, \\ \Lambda Y_{i2})t_k+\to Ga)4\Phi)t_k=2+, 3+, \\ SM\%7;)\Lambda Y_{i1})t_k+, \Lambda Y_{i2})t_k++\to C_{Clayton})F_1)\Lambda y_{i1})t_k++, F_2)\Lambda y_{i2})t_k++=3+, \\ \Lambda Y_{i1})t_k+\to N)2.6\Phi)t_k=2.3+, 1.6^2\Phi)t_k=2.3++, \\ \Lambda Y_{i2})t_k+\to Ga)4\Phi)t_k=2.3+, 3+, \\ \Lambda Y_{i2})t_k+\to Ga)4\Phi)t_k=2.5+, 3+, \\ \Lambda Y_{i3})t_k+\to Ga)4\Phi)t_k=2.5+, 3+, \\ \Lambda Y_{i4})t_k+\to Ga)4\Phi)t_k=2.5+, 3+, \\ \Lambda Y_{i4}(t_k+\to Ga)\Phi(t_k+\to G$$

Figures 5, 6, and 7 show the degradation paths of simulated data, as well as the contour plots of model densities for the degradation increments from 1 to 2 hour and from 2: to 31 hours. On each contour plot, the densities from both the true model and the estimated Wiener-Wiener model are depicted by using blue solid lines and green dashed lines for them, respectively. Based on these simulation results, several interesting findings can be drawn.

First, one can see that the bivariate degradation model that combines copula functions and stochastic process models is able to capture the dynamics of degradation process. This can be seen by the contour plots in two time phases. As shown by the degradation paths, the value of time scale transformation parameter, γ , directly determines the shape of degradation path. If γ [2, the degradation path indicates a linear trend over time as shown in Figure 6a. In other words, the degradation rate remains constant over the whole lifetime. However, if γ < 2, it demonstrates a concave trend as shown in Figure 5a, which has a decreasing degradation rate and is going to reach a saturation point eventually. On the contrary, Figure 7a shows a convex trend that exhibits accelerated deterioration. For a linear degradation process, its contour plots remain the same regardless of the phases of degradation. This can be observed from Figures 6b and 6c and this is because the parameters of marginal models do not change with the passage of time. But, for the case of SM%5, the density gradually moves to a border axis due to the slowdown of degradation process, as shown in Figures 5b and 5c.

One should also notice how the tail dependence is reflected in these figures. For example, since admitting only upper-tail dependence, the contour lines of Gumbel copula indicates a sharper shape

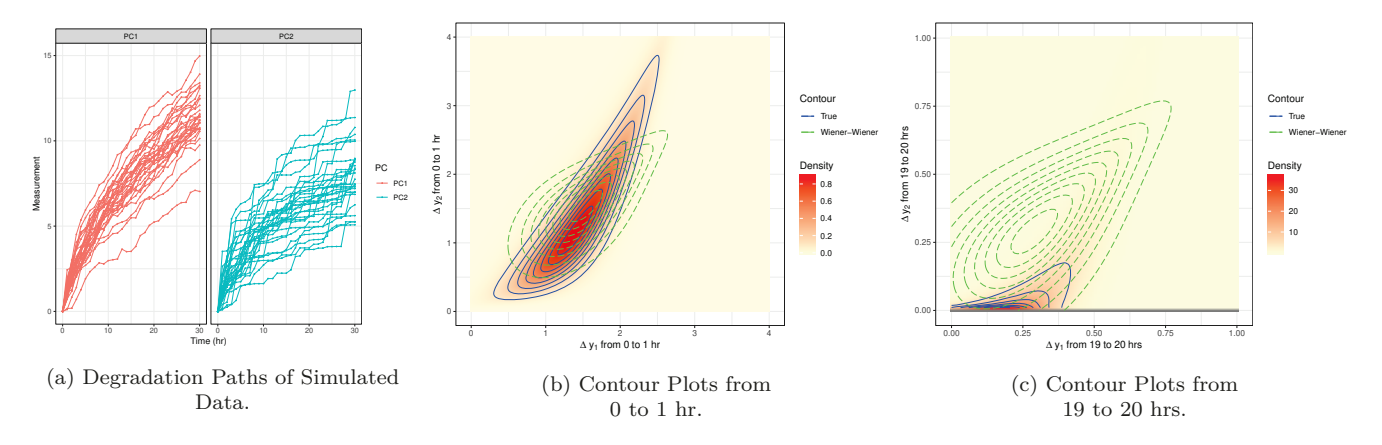


Figure 5: Monte Carlo Simulation Results for SM#4

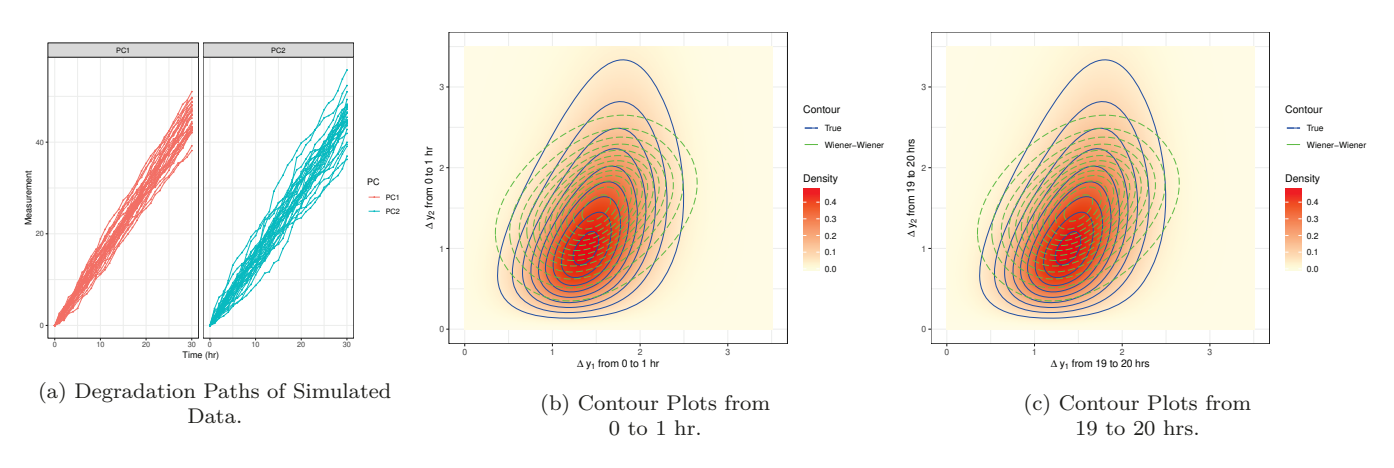


Figure 6: Monte Carlo Simulation Results for SM#5

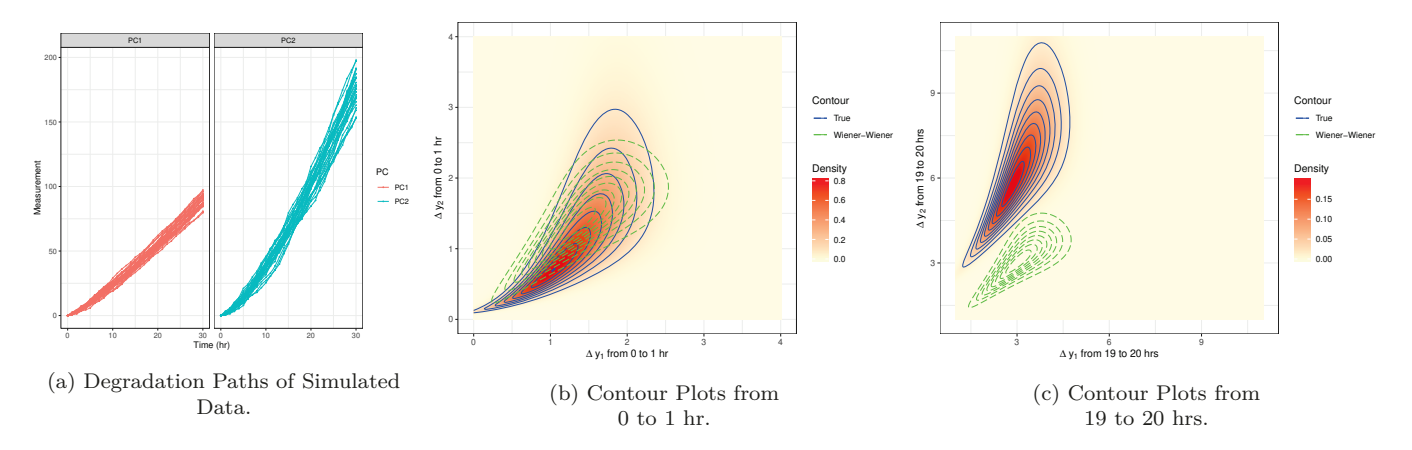


Figure 7: Monte Carlo Simulation Results for SM#6

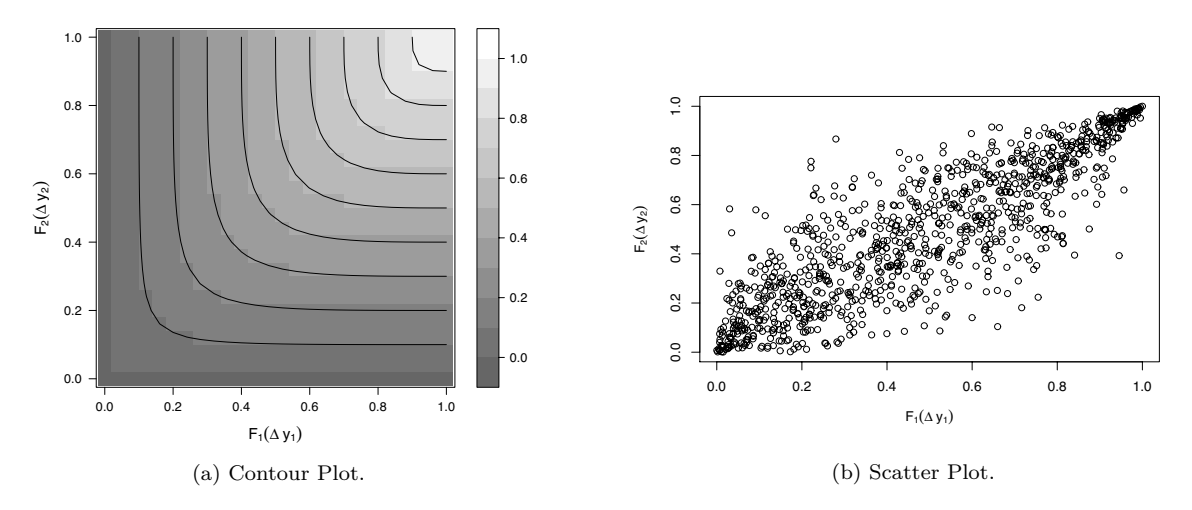


Figure 8: Simulated cdfs of Degradation Increments for SM#4.

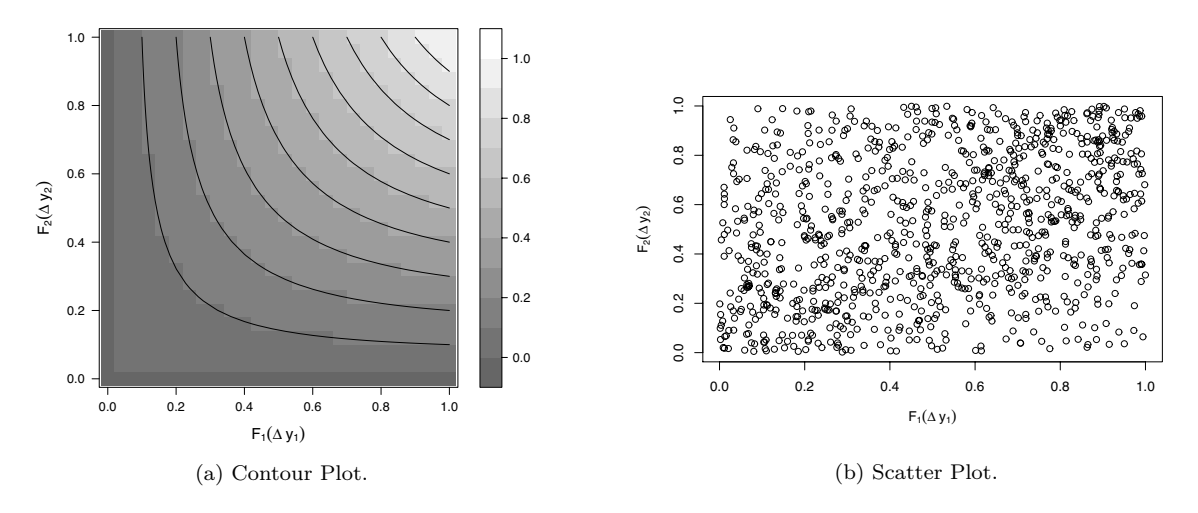


Figure 9: Simulated cdfs of Degradation Increments for SM#5.

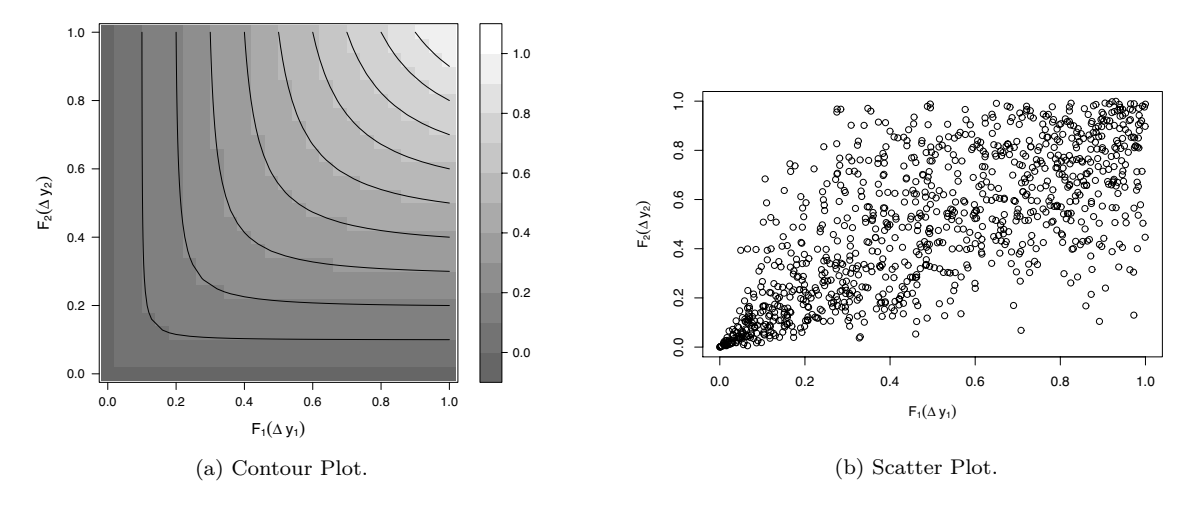


Figure 10: Simulated cdfs of Degradation Increments for SM#6.

in the upper right corner in Figure 5b. The same pattern is present in the lower left corner in Figure 7b for Clayton copula. To fully present such features, in Figures 8-10, we provide both the contour plots and scatter plots of cdfs of the degradation increments simulated from the three different copula models. As shown in Figure 8b, the simulated data points by SM%5 clustered around the right upper corner more compactly, where the pattern exists in the left lower corner as shown in Figure 10b. On the contrary, due to the symmetric feature of Frank copula, the simulated data points spread over the whole space, as shown in Figure 9b.

Lastly, and most importantly, it is noticed that if both marginals are decided to be Wiener processes a priori, the resulted joint density will be inconsistent with the true density. The difference will become larger and larger along the time if the degradation rate is not constant, because the time scale function will exaggerate the deficiency of a wrongly chosen model over time. For instance, in Figure 7b, the contour lines of the true model and the estimated model still overlap at the starting time, but they will be almost totally separated at the interval of 2: to 31 hours, as shown in Figure 7c. The Wiener-Wiener model would underestimate the degradation increment for y_2 by about 61(. Therefore, one can see that if the bivariate model is misspecified as a Wiener-Wiener combination, serious bias on the inference of the joint distribution would result. In such case, a misleading prediction of system reliability will be produced as well.

6. Applications

As we have shown, the proposed framework integrates the copula theory with general system reliability assessment, which allows for a straightforward interpretation of the multivariate model derived. Through the HMC-based Bayesian approach we proposed, the system reliability can be efficiently quantified. To apply the modeling framework to real examples, we design the following analysis procedure.

Step 1: Dependence Analysis

Given a degradation dataset, a nonparametric dependence analysis is first performed to check the rank correlation between two PCs. This step should be accompanied by the scatter plot function in most statistical software. If its rank correlation is high, a bivariate degradation model is needed for further quantitative analysis. Relevant implementations in R can be found in [54].

Step 2: Degradation Modeling and Parameters Estimation

Here, we build the bivariate degradation model as described in Section 4. Specifically, the two-stage Bayesian inference method is implemented to infer model parameters and to select the joint model.

Step 3: System Reliability Analysis

Finally, the system reliability analysis, as described in the lower part of Figure 3, can be carried out.

6.1. LED Degradation

In this example, we make use of the LED lamp dataset drawn from Chaluvadi's doctoral thesis [55]. This dataset presents a degradation testing result of LED lamps, of which lighting intensity is measured every 61 hours under a stress level of 51mA current. This dataset has also been analyzed by other researchers. For example, Ye et al. [56] and Tang et al. [44] did univariate modeling based on Wiener process, and Hao et al. [32] constructed a bivariate model using Frank copula with Gamma process as marginals.

To demonstrate the bivariate stochastic process modeling process, similarly to Hao et al. [32], we split the LED dataset into two streams as if the first half came from PC1 and the second half from

Table 2: LED Degradation Test Data.

	Inspection Time (hrs)									
Unit	0	50	100	150	200	250				
PC1										
1	100	86.6	78.7	76.0	71.6	68.0				
2	100	82.1	71.4	65.4	61.7	58.0				
3	100	82.7	70.3	64.0	61.3	59.3				
4	100	79.8	68.3	62.3	60.0	59.0				
5	100	75.1	66.7	62.8	59.0	54.0				
6	100	83.7	74.0	67.4	63.0	61.3				
PC2										
1	100	73.0	65.0	60.7	58.3	58.0				
2	100	86.2	67.6	62.7	60.0	59.7				
3	100	81.2	65.0	60.6	59.3	57.3				
4	100	66.8	63.3	59.3	57.3	56.5				
5	100	66.1	64.2	59.4	58.0	55.3				
6	100	76.5	61.7	61.3	59.7	56.0				

PC2. These data are shown in Table 2. A LED is considered to be failed if the PC1 value is below 20 or the PC2 value is below 40, which means ω_1 [91 and ω_2 [71. In addition, the degradation path of each PC for every unit is plotted in Figure 11a. Notice that it is necessary to apply a time scale transformation due to the nonlinear pattern of degradation path.

Step 1: According to the degradation path plot, one can see that the two PCs share a common change pattern. A dependence check, which computes the concordance between their negative increments, would further confirm this observation. As a result, the Kendall's coefficient of 1.6: indicates that there exists a strong dependency between the two PCs. Also, the scatter plot in Figure 11b exhibits a strong upper-tail dependency, as the regression slope becomes more prominent in the upper-right corner and it is flat for the data points in the lower-left corner.

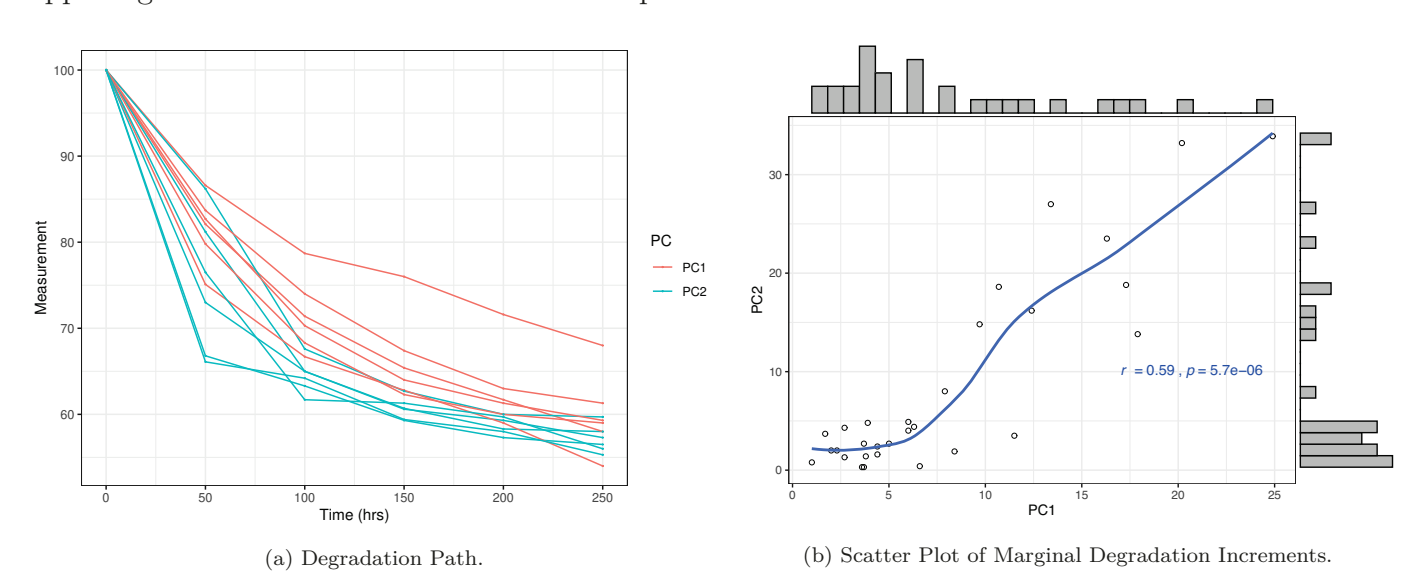


Figure 11: Degradation Path and Scatter Plot for LED Degradation Process.

Step 2: The first stage of parameter estimation for each PC is conducted on every MDPs described in Section 3.1. Their results are shown in Tables 3 and 4. Non-informative priors are utilized. To accommodate the nonlinear degradation pattern, we take use of the power transformation of Φ) $t=\gamma+[t^{\gamma}]$. The low BIC values of Gamma process indicate that this stochastic process model is suitable for both PCs.

Table 3: Parameters Estimation for Marginal Models of PC1.

MDP	Parameter	mean	se_mean	sd	2.5%	97.5%	BIC
Wiener	α	3.493	0.022	0.750	2.974	5.268	
Process	β	1.734	0.009	0.342	1.494	2.519	146.641
	γ	0.446	0.001	0.037	0.371	0.518	
Gamma	α	3.682	0.029	1.255	1.563	6.508	
Process	β	1.131	0.007	0.299	0.607	1.777	145.055
	γ	0.459	0.001	0.037	0.391	0.539	_
IG	α	3.398	0.022	0.722	2.124	4.913	
Process	β	11.117	0.178	5.589	2.861	25.563	147.010
	γ	0.452	0.001	0.037	0.386	0.524	

Table 4: Parameters Estimation for Marginal Models of PC2.

MDP	Parameter	mean	se_mean	sd	2.5%	97.5%	BIC
Wiener	α	9.350	0.098	3.101	4.744	16.969	
Process	β	5.678	0.052	1.638	3.522	9.709	182.730
	γ	0.284	0.002	0.054	0.177	0.391	
Gamma	α	2.695	0.029	1.111	0.905	5.194	
Process	β	0.347	0.002	0.096	0.184	0.559	164.682
	γ	0.320	0.001	0.052	0.229	0.434	
IG	α	8.854	0.079	2.673	4.335	14.742	
Process	β	17.492	0.368	12.902	2.279	48.242	166.091
	γ	0.301	0.002	0.051	0.215	0.412	

Based on the estimation of MDP model parameters, the corresponding cdf of individual PC's degradation increments are obtained as $(F_1)\Lambda y_{i1}(t_k+,F_2)\Lambda y_{i2}(t_k+,F_2)\Lambda y_{i2}(t_k+,F_2)\Lambda$

Table 5: Parameters Estimation for Joint Models.

		Joint							
Copula	Parameter	mean	se_mean	sd	2.5%	97.5%	au	BIC	
Joe	δ	1.899	0.010	0.357	1.263	2.652	0.332	-5.632	
Frank	δ	2.201	0.030	1.167	-0.056	4.628.	0.234	0.944	
Gumbel	δ	1.443	0.006	0.202	1.096	1.889	0.307	-2.346	
Clayton	δ	0.131	0.006	0.211	-0.191	0.601	0.061	4.125	

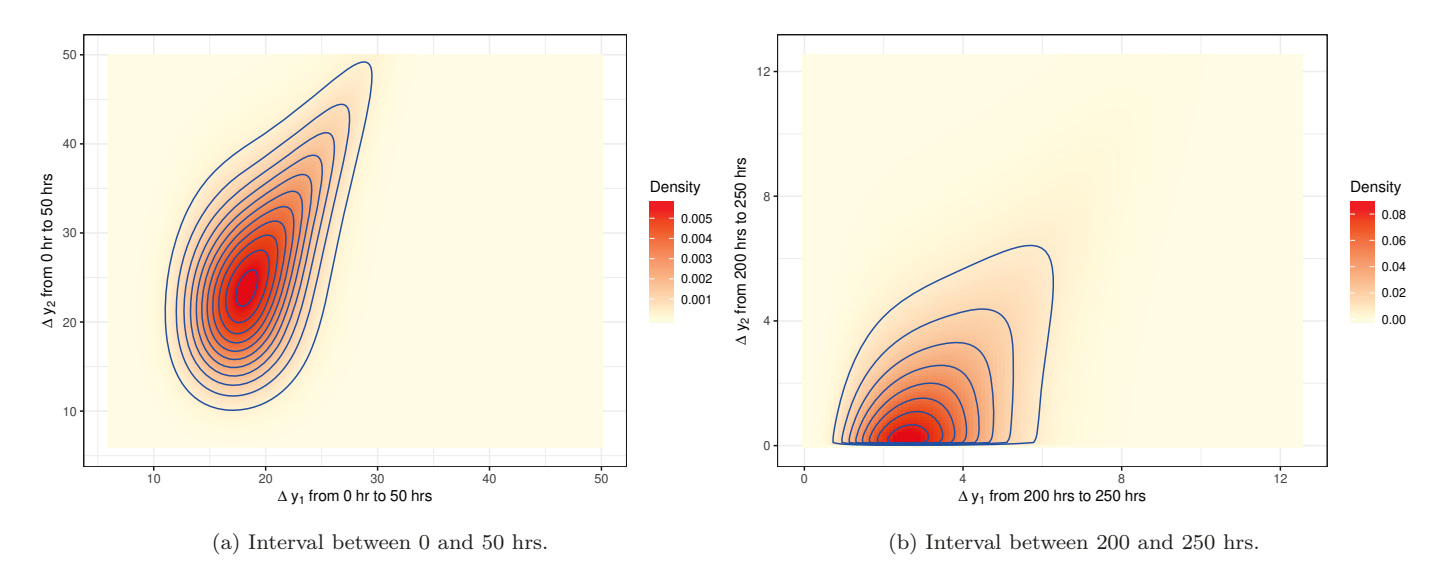


Figure 12: Contour Plots of Joint Distribution Density of Degradation Increments.

Step 3: Finally, through implementing the procedure of reliability estimation presented in Figure 3, median curves of reliability prediction over the duration of 1 to 4,111 hours for both the marginal and joint distributions are plotted in Figure 13. As a comparison, the case of independence of two PCs is also presented. It is noted that the independence assumption would underestimate the product's reliability. For instance, at 2,111 hours, the predicted reliability using Joe copula is about 1.3, but it will be 36(less if the two PCs are assumed to be independent. This result is not a surprise because Theorem 1 has shown that $\int_{j=1}^{M} R_j t_j + \sum_{j=1}^{M} R_j t_j + \sum$

6.2. Polymeric Material Degradation

In this section, we revisit the motivating example to demonstrate the advantage of the proposed general bivariate degradation model with the incorporation of covariates.

Step 1: As stated in Section 1.2, the two PCs, benzene ring mass loss and aromatric C-O are named as PC1 and PC2. Observing that the degradation paths of both PCs share similar patterns, it is necessary to evaluate their dependency to each other. Since the degradation path is also affected by some external environmental factors, such as temperature and UV intensity in this example, we have to evaluate the dependency at the same environmental stress level. We calculate the Kendall's coefficient of the degradation increments of both PCs for each test unit and compute the average value at each stress level. It is found that the Kendall's τ remains around 1.69 across all stress levels, as shown in Figure 15.

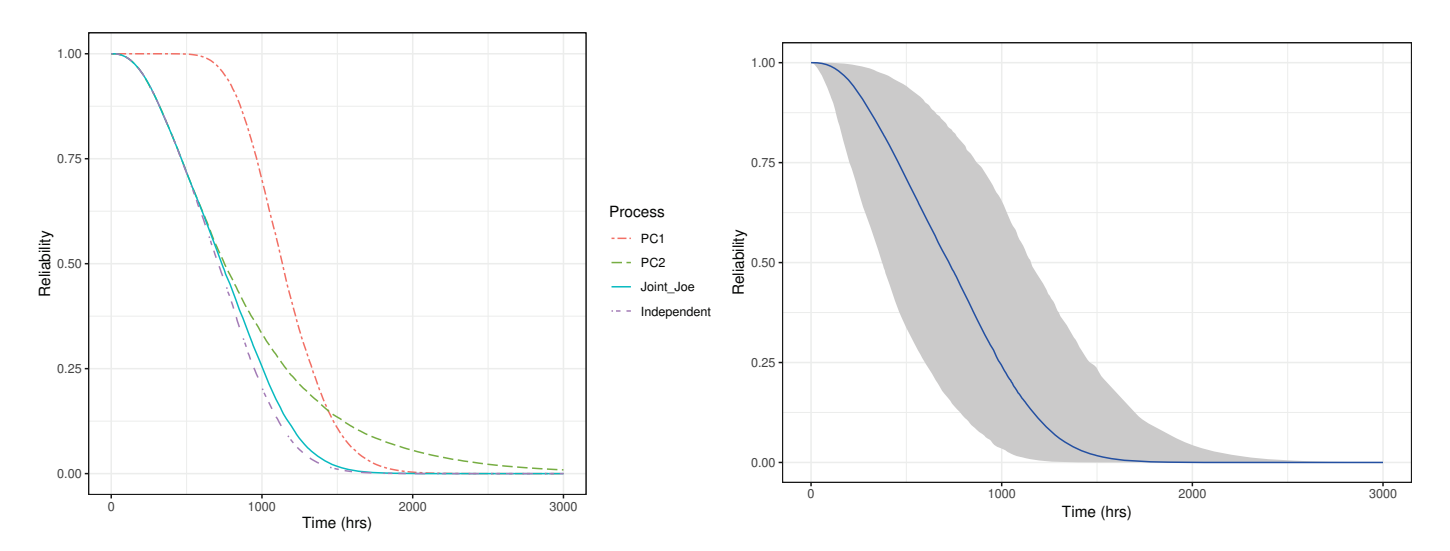


Figure 13: Reliability Curves for LED Degradation Process.

Figure 14: 95% Credible Band for Reliability Curve by Joe Copula.

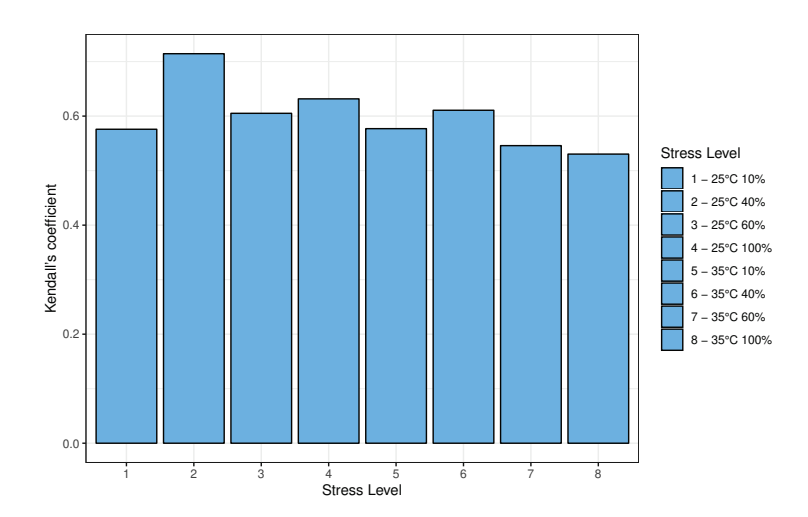


Figure 15: Barchart of Average Kendall's tau at Each Stress Level.

Step 2: Following the dependence analysis, we fit MDPs to each PC's degradation dataset. The Arrhenius relation is chosen to incorporate the degradation acceleration effect brought by temperature and a power law relation is used to model the effect by UV intensity [16]. Taking the Wiener process as example, the drift parameter can be written as

$$\alpha g \times \eta_1 \frac{22716}{TEMP \ 0 \ 384.26} \left[ND^{\eta_2} \Lambda \Phi t = \gamma + \right]$$

Tables 6 and 7 show the parameters estimation of marginal models for both PCs. It turns out that Gamma process is the best model for each PC.

The second stage of parameter inference is carried out by considering the four candidate copulas listed in Section 2.2. The results in Table 8 indicate that Gumbel copula is the best model. Similarly to the previous example, we provide the contour plot of joint distribution density of degradation increments in Figure 16. This is done by assuming a stress level of TEMP 30°C and UV Intensity 85%. It can be seen that the two contour plots do not differ much for two different durations because the parameter γ is close to 2.

 ${\bf Table~6:~Parameters~Estimation~for~Marginal~Models~of~PC1.}$

				PC1			
MDP	Parameter	mean	se_mean	sd	2.5%	97.5%	BIC
Wiener	α	480.082	13.260	431.709	162.646	1634.755	
Process	β	$0.245 \equiv 21^{-2}$	0.000	$0.017 \equiv 21^{-2}$	$0.215 \equiv 21^{-2}$	$0.280 \equiv 21^{-2}$	
	η_1	$-37.545 \equiv 21^{-2}$	$0.780 \equiv 21^{-3}$	$2.602 \equiv 21^{-2}$	$-41.938 \equiv 21^{-2}$	$-32.173 \equiv 21^{-2}$	-11,808.679
	η_2	$30.227 \equiv 21^{-2}$	$0.720 \equiv 21^{-3}$	$3.892 \equiv 21^{-2}$	$22.968 \equiv 21^{-2}$	$38.242 \equiv 21^{-2}$	
	γ	$121.228 \equiv 21^{-2}$	$0.590 \equiv 21^{-3}$	$2.478 \equiv 21^{-2}$	$116.324 \equiv 21^{-2}$	$126.027 \equiv 21^{-2}$	_
Gamma	α	1220.323	14.889	778.138	247.657	3269.224	-
Process	β	271.281	$14.549 \equiv 21^{-2}$	$966.653 \equiv 21^{-2}$	251.713	290.697	
	η_1	$-21.360 \equiv 21^{-2}$	$0.360 \equiv 21^{-3}$	$1.707 \equiv 21^{-2}$	$-24.456 \equiv 21^{-2}$	$-17.730 \equiv 21^{-2}$	-12,299.737
	η_2	$24.734 \equiv 21^{-2}$	$0.260 \equiv 21^{-3}$	$1.737 \equiv 21^{-2}$	$21.411 \equiv 21^{-2}$	$28.087 \equiv 21^{-2}$	
	γ	$93.633 \equiv 21^{-2}$	$0.190 \equiv 21^{-3}$	$1.256 \equiv 21^{-2}$	$91.225 \equiv 21^{-2}$	$96.082 \equiv 21^{-2}$	
IG	α	48.880≡21 ²	$1.286 \equiv 21^{-2}$	$41.116 \equiv 21^{-2}$	6.799=21 ²	$155.859 \equiv 21^{-2}$	-
Process	β	60.323	3.811	135.520	0.678	364.094	
	η_1	$-13.572 \equiv 21^{-2}$	$0.660 \equiv 21^{-3}$	$2.051 \equiv 21^{-2}$	$-17.343 \equiv 21^{-2}$	$-9.337 \equiv 21^{-2}$	-11,555.913
	η_2	$19.127 \equiv 21^{-2}$	$0.330 \equiv 21^{-3}$	$1.654 \equiv 21^{-2}$	$16.024 \equiv 21^{-2}$	$22.364 \equiv 21^{-2}$	
	γ	$85.653 \equiv 21^{-2}$	$0.190 \equiv 21^{-3}$	$0.963 \equiv 21^{-2}$	$83.769 \equiv 21^{-2}$	$87.535 \equiv 21^{-2}$	

Table 7: Parameters Estimation for Marginal Models of PC2.

	PC2							
MDP	Parameter	mean	se_mean	sd	2.5%	97.5%	BIC	
Wiener	α	531.736	15.829	480.608	30.187	1775.501		
Process	β	$0.167 \equiv 21^{-2}$	0.000	$0.011 \equiv 21^{-2}$	$0.146 \equiv 21^{-2}$	$0.191 \equiv 21^{-2}$		
	η_1	$-41.780 \equiv 21^{-2}$	$0.088 \equiv 21^{-2}$	$2.850 \equiv 21^{-2}$	$-46.307 \equiv 21^{-2}$	$-35.574 \equiv 21^{-2}$	-10,637.895	
	η_2	$38.013 \equiv 21^{-2}$	$0.091 \equiv 21^{-2}$	$4.719 \equiv 21^{-2}$	$29.106 \equiv 21^{-2}$	$47.285 \equiv 21^{-2}$		
	γ	$149.189 \equiv 21^{-2}$	$0.056 \equiv 21^{-2}$	$2.567 \equiv 21^{-2}$	$144.189 \equiv 21^{-2}$	$154.199 \equiv 21^{-2}$		
Gamma	α	903.878	12.225	646.404	165.343	2653.679		
Process	β	199.416	0.114	7.067	185.498	213.338		
	η_1	$-23.848 \equiv 21^{-2}$	$0.040 \equiv 21^{-2}$	$1.853 \equiv 21^{-2}$	$-27.295 \equiv 21^{-2}$	$-19.937 \equiv 21^{-2}$	-11,467.287	
	η_2	$34.345 \equiv 21^{-2}$	$0.029 \equiv 21^{-2}$	$1.909 \equiv 21^{-2}$	$30.550 \equiv 21^{-2}$	$38.002 \equiv 21^{-2}$		
	γ	$109.679 \equiv 21^{-2}$	$0.024 \equiv 21^{-2}$	$1.535 \equiv 21^{-2}$	$106.726 \equiv 21^{-2}$	$112.708 \equiv 21^{-2}$		
IG	α	$44.905 \equiv 21^{-2}$	$1.021 \equiv 21^{-2}$	$39.051 \equiv 21^{-2}$	$6.625 \equiv 21^{-2}$	$154.426 \equiv 21^{-2}$	-	
Process	β	38.849	2.034	85.222	0.492	265.431		
	η_1	$-16.242 \equiv 21^{-2}$	$0.060 \equiv 21^{-2}$	$2.103 \equiv 21^{-2}$	$-20.293 \equiv 21^{-2}$	$-12.078 \equiv 21^{-2}$	-10,867.262	
	η_2	$34.479 \equiv 21^{-2}$	$0.032 \equiv 21^{-2}$	$1.674 \equiv 21^{-2}$	$31.221 \equiv 21^{-2}$	$37.774 \equiv 21^{-2}$		
	γ	$100.229 \equiv 21^{-2}$	$0.021 \equiv 21^{-2}$	$1.091 \equiv 21^{-2}$	$98.166 \equiv 21^{-2}$	$102.466 \equiv 21^{-2}$		

Table 8: Parameters Estimation of Joint Models.

Copula	Parameter	mean	se_mean	sd	2.5%	97.5%	au	BIC
Joe	δ	3.290	0.002	0.078	3.138	3.446	0.551	-2,408.710
Frank	δ	10.361	0.006	0.249	9.869	10.850	0.675	-2,572.549
Gumbel	δ	2.724	0.001	0.050	2.627	2.825	0.633	-3,043.961
Clayton	δ	1.256	0.001	0.049	1.161	1.353	0.386	-1,560.568

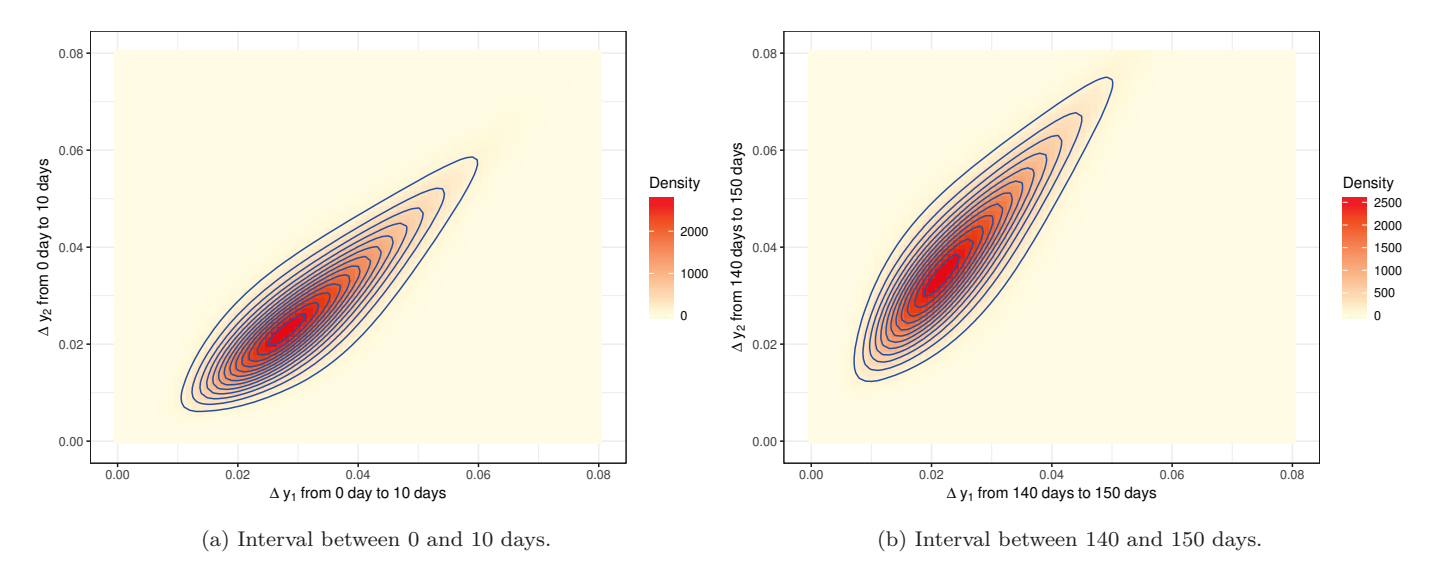


Figure 16: Contour Plots of Joint Distribution Density of Degradation Increments at TEMP 30 °C and UV Intensity 85%.

Step 3: Lastly, we provide the point and interval predictions of reliability for the duration of the first 611 days. For the polymeric degradation data, we use a threshold ω_1 [1.5 and ω_2 [1.6 for PC1 and PC2, respectively, and treat it as a serial system. Correspondingly, Figure 17 shows the reliability curves for both marginal processes and joint models. Again, if the two PCs are assumed to be independent to each other, the resulting reliability prediction will be below the level when they are correlated. Specially, we compare the material's reliability under two different environmental conditions – TEMP 30 °C and UV Intensity 85% v.s. TEMP 20 °C and UV Intensity 50%. One may regard these two conditions as one in Phoenix, AZ (where the weather is sunny and hot) and the other one in Raleigh, NC (where the weather is mild). The polymeric material's lifetime in Raleigh is expected to be longer. The median lifetime in Phoenix (see Figure 18a) is about 281 days, while in Raleigh it will be more than 211 days longer (see Figure 18b). It is also obvious that, due to having more degradation data available in this example, the : 6(credible band is much narrower here than the previous example.

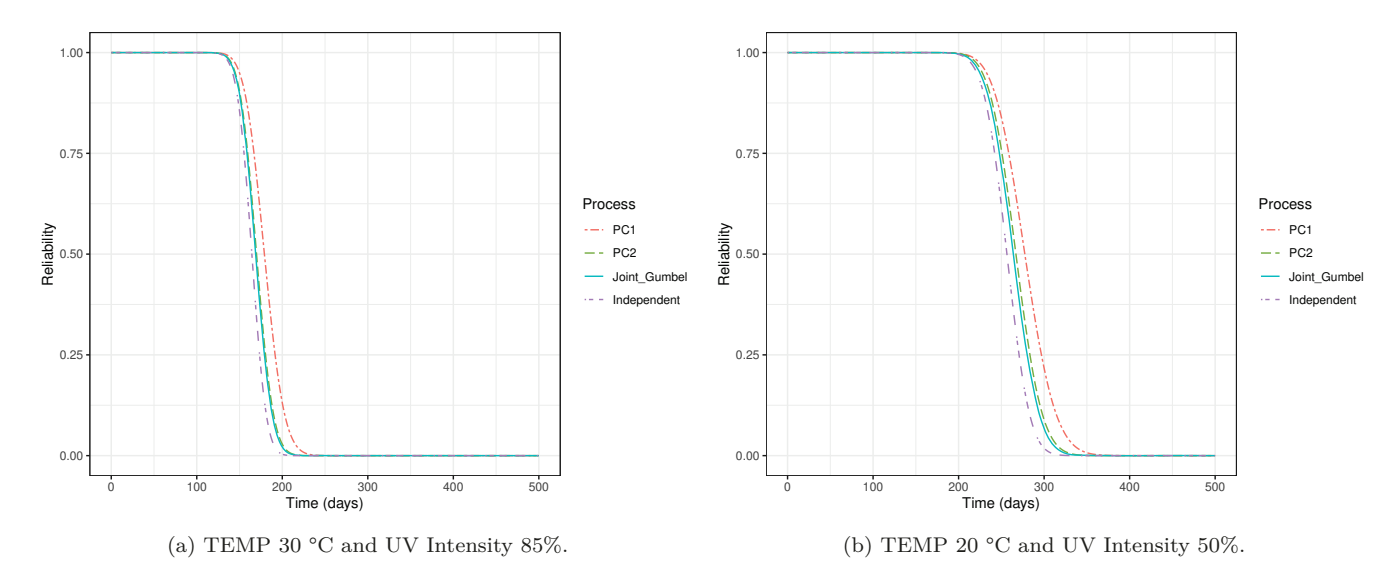


Figure 17: Reliability Curves for Polymeric Degradation Process.

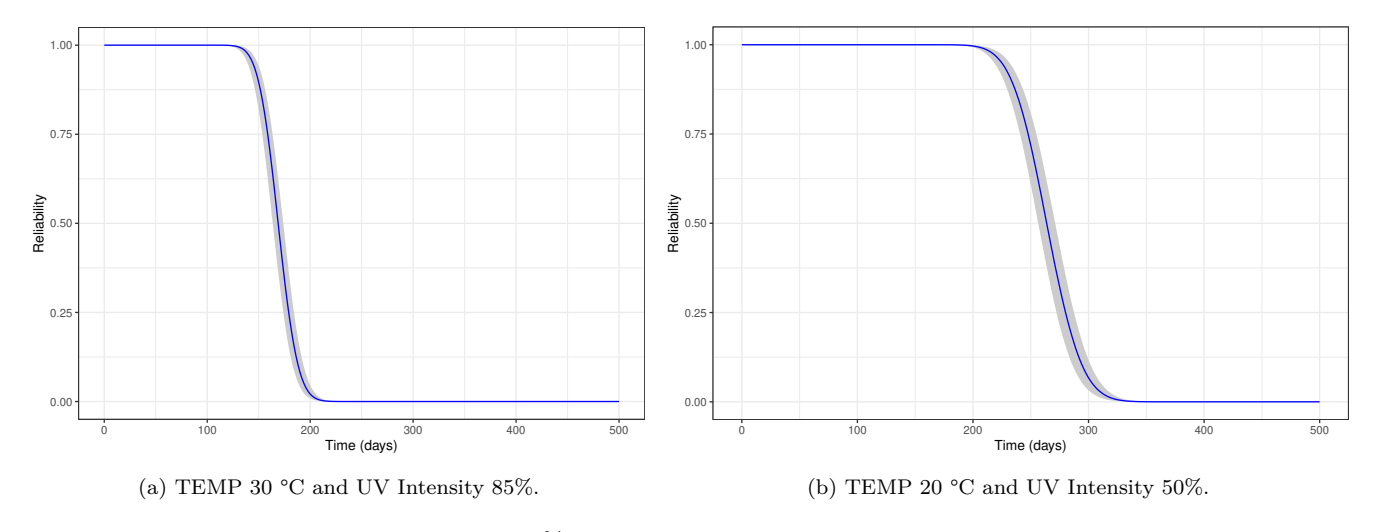


Figure 18: 95% Credible Band for Reliability Curve.

7. Conclusions

A degrading system may involve multiple components or PCs that apparently have interactions or share a common failure mechanism. In such case, cares must be taken to consider the PC dependency when we analyze system reliability. In previous research, the choice of bivariate joint distribution was often pre-determined, which was unfortunately inappropriate in most cases, especially when the marginals are subject to different distributions. By introducing copula functions, we are able to provide a complete theoretical framework to investigate the effect of PC dependency on system reliability. Within this modeling framework, a flexible class of bivariate stochastic process-based degradation models are proposed and they include a variety of marginal degradation processes and incorporate stress covariates. In addition, an efficient Bayesian inference method, HMC, is implemented in this paper, which is novel for degradation data analysis. The consequences of model misspecification are thoroughly studied in Section 5.2. The different types of tail dependence of copula functions that mimic bivariate degradation patterns are discussed too. Two real examples are used to demonstrate the superiority of our approach.

Beyond the scope of current study, there are several other issues worth of a further investigation. For instance, it is our interest to investigate the inference method when some random effects accounting for the unit-to-unit variation are included in the model. Endowing the analysis with a goodness-of-fit test on multivariate degradation models is intended to be conducted too. This task is not easy; but tailored test statistics are possible to be built based on several existing test methods about copulas, such as the Cramér-von Mises statistic [57]. Also, how to model a system with multiple components in a complex structure or a multi-component system with multiple PCs requires an extensive research. Moreover, the extension of the current work to a more general setting, such as incorporating both time-to-failure data and binary pass-fail data, need be further developed.

Acknowledgement

The research by the first and second authors were partially supported by NSF grant 1726445 and the research by the third author was partially supported by NSF grant 1838271.

Appendix: Proof of Theorem 1

Here, we prove the case of serial system, that is

$$r_j^M R_j(t) + \geq R_s(t) + \geq n \log(R_1)t + R_2(t) + \ldots, R_M(t) + \ldots$$

For the case of parallel system, it is omitted due to similar steps.

First, the upper bound is intuitive since the system would fail if any component had failed. This is obvious because of the serial structure and the property of coherent system.

Then, to prove $\int_{j=1}^{M} R_j t + \langle R_s \rangle t +$ This is equivalent to prove

$$P(Y_1)t + <\omega_1, Y_2)t + <\omega_2, \dots, Y_M)t + <\omega_M + \sim$$

$$P(Y_1)t + <\omega_1 + P(Y_2)t + <\omega_2 + = \times \times = P(Y_M)t + <\omega_M + <\omega_M + P(Y_M)t + <\omega_M + <\omega_M$$

According to **Definition 1**, a random d-vector, X, is positively associated if the inequality

$$E[q_1)X+q_2)X+\sim E[q_1)X+E[q_2)X+$$

holds for all real-value functions g_1 and g_2 , which are increasing (in each component) and their expectations exist. Also, a random subvector of X is also positively associated.

Thus, we can treat $Y(t+[]Y_1(t+Y_2(t+\ldots,Y_M(t+T))]$ as a random vector and let

$$g_1)y_1)t+y_2)t+\dots,y_{M-1})t++[I_{(-\omega_1)*(-\omega_2)*(-\omega_2)*(-\omega_{M-1})})y_1)t+y_2)t+\dots,y_{M-1})t++\dots$$
 $g_2)y_M)t++[I_{(-\omega_M)})y_M)t+\dots$

The above inequality leads to

$$P(Y_1)t + <\omega_1, Y_2)t + <\omega_2, \dots, Y_M)t + <\omega_M + \sim \\ P(Y_1)t + <\omega_1, Y_2)t + <\omega_2, \dots, Y_{M-1})t + <\omega_{M-1} + \equiv P(Y_M)t + <\omega_M + \infty$$

By induction, it can be shown that the lower bound in **Theorem 1** holds. \square

Supplementary Materials

The supplementary materials (a PDF file) include the information of the priors used for all model parameters, the simulation results, and the diagnostic plots of statistical inference for two examples presented in this paper.

References

- [1] Z. Pan, Q. Sun, J. Feng, Reliability modeling of systems with two dependent degrading components based on Gamma processes, Communications in Statistics-Theory and Methods 45 (2016) 1923–1938.
- [2] W. Q. Meeker, L. A. Escobar, Statistical Methods for Reliability Data, John Wiley & Sons, Inc., New York, 1998.
- [3] S. J. Bae, P. H. Kvam, A nonlinear random-coefficients model for degradation testing, Technometrics 46 (2004)
- [4] R. Pan, T. Crispin, A hierarchical modeling approach to accelerated degradation testing data analysis: A case study, Quality and Reliability Engineering International 27 (2011) 229–237.
- [5] Y. Xing, E. W. Ma, K.-L. Tsui, M. Pecht, An ensemble model for predicting the remaining useful performance of lithium-ion batteries, Microelectronics Reliability 53 (2013) 811 820.

- [6] G. Fang, S. E. Rigdon, R. Pan, Predicting lifetime by degradation tests: A case study of ISO 10995, Quality and Reliability Engineering International 34 (2018) 1228–1237.
- [7] G. A. Whitmore, Estimation degradation by a Wiener diffusion process subject to measurement error, Lifetime Data Analysis 1 (1995) 307–319.
- [8] Y. Wen, J. Wu, D. Das, T.-L. B. Tseng, Degradation modeling and RUL prediction using Wiener process subject to multiple change points and unit heterogeneity, Reliability Engineering & System Safety 176 (2018) 113–124.
- [9] H. Gao, L. Cui, D. Kong, Reliability analysis for a Wiener degradation process model under changing failure thresholds, Reliability Engineering & System Safety 171 (2018) 1–8.
- [10] C. Park, W. J. Padgett, Accelerated degradation models for failure based on Geometric Brownian motion and Gamma processes, Lifetime Data Analysis 11 (2005) 511–527.
- [11] M. E. Cholette, H. Yu, P. Borghesani, L. Ma, G. Kent, Degradation modeling and condition-based maintenance of boiler heat exchangers using Gamma processes, Reliability Engineering & System Safety 183 (2019) 184–196.
- [12] Q. Dong, L. Cui, A study on stochastic degradation process models under different types of failure thresholds, Reliability Engineering & System Safety 181 (2019) 202–212.
- [13] Z.-S. Ye, N. Chen, The Inverse Gaussian process as a degradation model, Technometrics 56 (2014) 302–311.
- [14] X. Wang, D. Xu, An Inverse Gaussian process model for degradation data, Technometrics 52 (2010) 188–197.
- [15] C.-Y. Peng, Inverse Gaussian processes with random effects and explanatory variables for degradation data, Technometrics 57 (2016) 100–111.
- [16] I. Vaca-Trigo, W. Q. Meeker, A statistical model for linking field and laboratory exposure results for a model coating, in: Service life prediction of polymeric materials, Springer, 2009, pp. 29–43.
- [17] X. Gu, D. Stanley, W. E. Byrd, B. Dickens, I. Vaca-Trigo, W. Q. Meeker, T. Nguyen, J. W. Chin, J. W. Martin, Linking accelerated laboratory test with outdoor performance results for a model epoxy coating system, in: Service Life Prediction of Polymeric Materials, Springer, 2009, pp. 3–28.
- [18] Y. Duan, Y. Hong, W. Q. Meeker, D. L. Stanley, X. Gu, Photodegradation modeling based on laboratory accelerated test data and predictions under outdoor weathering for polymeric materials, Annals of Applied Statistics 11 (2017) 2052–2079.
- [19] Y. Hong, M. Zhang, W. Q. Meeker, Big data and reliability applications: The complexity dimension, Journal of Quality Technology 50 (2018) 135–149.
- [20] Y. Hong, Y. Duan, W. Q. Meeker, D. L. Stanley, X. Gu, Statistical methods for degradation data with dynamic covariates information and an application to outdoor weathering data, Technometrics 57 (2015) 180–193.
- [21] P. Wang, D. W. Coit, Reliability prediction based on degradation modeling for systems with multiple degradation measures, in: Proceedings of the 2004 Reliability and Maintainability Symposium, 2004, pp. 302–307.
- [22] Z. Pan, N. Balakrishnan, Reliability modeling of degradation of products with multiple performance characteristics based on Gamma processes, Reliability Engineering & System Safety 96 (2011) 949–957.
- [23] X. Wang, N. Balakrishnan, B. Guo, P. Jiang, Residual life estimation based on bivariate non-stationary Gamma degradation process, Journal of Statistical Computation and Simulation 85 (2015) 405–421.
- [24] W. Si, Q. Yang, X. Wu, Y. Chen, Reliability analysis considering dynamic material local deformation, Journal of Quality Technology 50 (2018) 183–197.
- [25] G. Fang, R. Pan, Y. Hong, A copula-based multivariate degradation analysis for reliability prediction, in: 2018 Annual Reliability and Maintainability Symposium (RAMS), 2018, pp. 1–7. doi:10.1109/RAM.2018.8463026.
- [26] D. Lee, R. Pan, A nonparametric bayesian network approach to assessing system reliability at early design stages, Reliability Engineering & System Safety 171 (2018) 57–66.
- [27] W. Peng, Y.-F. Li, Y.-J. Yang, S.-P. Zhu, H.-Z. Huang, Bivariate analysis of incomplete degradation observations based on Inverse gaussian processes and copulas, IEEE Transactions on Reliability 65 (2016) 624–639.
- [28] Z. Pan, N. Balakrishnan, Q. Sun, J. Zhou, Bivariate degradation analysis of products based on wiener processes and copulas, Journal of Statistical Computation and Simulation 83 (2013) 1316–1329.
- [29] W. Peng, Y.-F. Li, J. Mi, L. Yu, H.-Z. Huang, Reliability of complex systems under dynamic conditions: A bayesian multivariate degradation perspective, Reliability Engineering and System Safety 153 (2016) 75–87.
- [30] L. A. Rodríguez-Picón, V. H. Flores-Ochoa, L. C. Méndez-González, M. A. Rodríguez-Medina, Bivariate degradation modelling with marginal heterogeneous stochastic processes, Journal of Statistical Computation and Simulation 87 (2017) 2207–2226.
- [31] W. Peng, Z. Ye, N. Chen, Joint online RUL prediction for multivariate deteriorating systems, IEEE Transactions on Industrial Informatics 15 (2019) 2870–2878.
- [32] H. Hao, C. Su, C. Li, LED lighting system reliability modeling and inference via random effects Gamma process and copula function, International Journal of Photoenergy 2015 (2015).
- [33] H. Joe, Multivariate models and multivariate dependence concepts, Chapman and Hall/CRC, 1997.

- [34] R. B. Nelsen, An introduction to copulas, Springer Science & Business Media, 2007.
- [35] P. Jaworski, F. Durante, W. K. Hardle, T. Rychlik, Copula theory and its applications, volume 198, Springer, 2010.
- [36] C. Li, V. P. Singh, A. K. Mishra, A bivariate mixed distribution with a heavy-tail LED component and its application to single-site daily rainfall simulation, Water Resources Research 49 (2013) 767–789.
- [37] Z.-S. Ye, M. Xie, Stochastic modelling and analysis of degradation for highly reliable products, Applied Stochastic Models in Business and Industry 31 (2015) 16–32.
- [38] K.-i. Sato, S. Ken-Iti, Lévy processes and infinitely divisible distributions, Cambridge university press, 1999.
- [39] W. Nelson, Accelerated Testing: Statistical Models, Test Plans, and Data Analyses, (Republished in a paperback in Wiley Series in Probability and Statistics, 2004), John Wiley & Sons, New York, 1990.
- [40] K. A. Doksum, S.-L. T. Normand, Gaussian models for degradation processes-part i: Methods for the analysis of biomarker data, Lifetime Data Analysis 1 (1995) 131–144.
- [41] L.-C. Tang, G. Yang, M. Xie, Planning of step-stress accelerated degradation test, in: Reliability and Maintain-ability, 2004 Annual Symposium-RAMS, IEEE, 2004, pp. 287–292.
- [42] W. J. Padgett, M. A. Tomlinson, Inference from accelerated degradation and failure data based on Gaussian process models, Lifetime Data Analysis 10 (2004) 191–206.
- [43] C.-M. Liao, S.-T. Tseng, Optimal design for step-stress accelerated degradation tests, IEEE Transactions on Reliability 55 (2006) 59–66.
- [44] S. Tang, X. Guo, C. Yu, H. Xue, Z. Zhou, Accelerated degradation tests modeling based on the nonlinear wiener process with random effects, Mathematical Problems in Engineering 2014 (2014).
- [45] F. Sun, L. Liu, X. Li, H. Liao, Stochastic modeling and analysis of multiple nonlinear accelerated degradation processes through information fusion, Sensors 16 (2016) 1242.
- [46] J. L. Folks, R. S. Chhikara, The inverse gaussian distribution and its statistical application—a review, Journal of the Royal Statistical Society. Series B (Methodological) (1978) 263–289.
- [47] H. Joe, Asymptotic efficiency of the two-stage estimation method for copula-based models, Journal of Multivariate Analysis 94 (2005) 401–419.
- [48] H. Hao, C. Su, A Bayesian framework for reliability assessment via Wiener process and MCMC, Mathematical Problems in Engineering 2014 (2014).
- [49] P. D. Hoff, A first course in Bayesian statistical methods, Springer Science & Business Media, 2009.
- [50] D. J. Lunn, A. Thomas, N. Best, D. Spiegelhalter, Winbugs-a Bayesian modelling framework: concepts, structure, and extensibility, Statistics and computing 10 (2000) 325–337.
- [51] S. Brooks, A. Gelman, G. Jones, X.-L. Meng, Handbook of Markov Chain Monte Carlo, CRC press, 2011.
- [52] C. C. Monnahan, J. T. Thorson, T. A. Branch, Faster estimation of Bayesian models in ecology using Hamiltonian Monte Carlo, Methods in Ecology and Evolution 8 (2017) 339–348.
- [53] B. Carpenter, A. Gelman, M. D. Hoffman, D. Lee, B. Goodrich, M. Betancourt, M. Brubaker, J. Guo, P. Li, A. Riddell, Stan: A probabilistic programming language, Journal of Statistical Software 76 (2017).
- [54] M. Hofert, Elements of Copula Modeling with R, Springer, 2018.
- [55] V. N. H. Chaluvadi, Accelerated life testing of electronic revenue meters, Ph.D. thesis, Clemson University, 2008.
- [56] Z.-S. Ye, Y. Wang, K.-L. Tsui, M. Pecht, Degradation data analysis using wiener processes with measurement errors, IEEE Transactions on Reliability 62 (2013) 772–780.
- [57] C. Genest, B. Rémillard, D. Beaudoin, Goodness-of-fit tests for copulas: A review and a power study, Insurance: Mathematics and economics 44 (2009) 199–213.